Plasma Science & Fusion Center

Steady-state core performance optimization with physics-based models for SPARC and ARC

A. Saltzman[1,*], P. Rodriguez-Fernandez[1], A. Ho[1], M.S. Anastopoulos Tzanis[2], G. Snoep[1], J. Han[1], J. Hall[1], K. Yanna[1], J. Hillesheim[3], T. Body[3], A.J. Creely[3], P. Snyder[3], N.T. Howard[1]

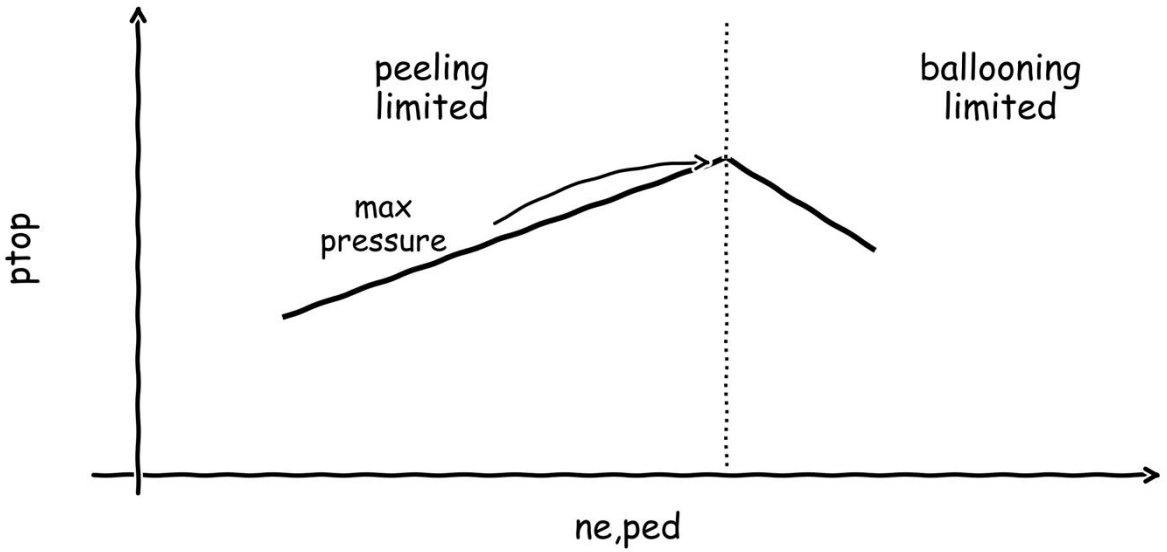
*audreysa@mit.edu [1]MIT PSFC [2]Oak Ridge National Lab [3]Commonwealth Fusion Systems

This work is supported by Commonwealth Fusion Systems, under RPP020. The authors acknowledge the MIT Office of Research Computing and Data for providing high-performance computing resources. ChatGPT, Claude, and Gemini assisted in code and figure generation.

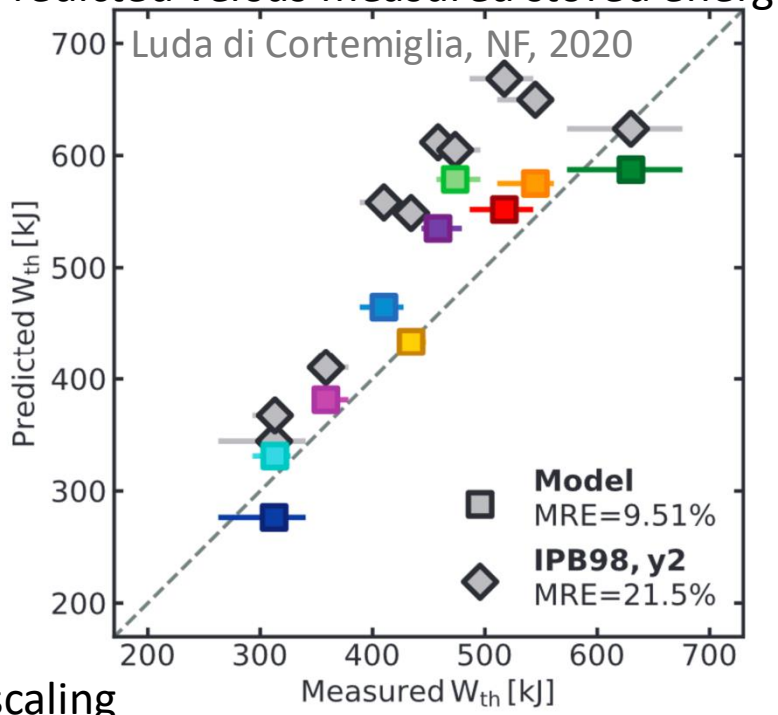
Physics-based models can make more accurate fusion performance predictions than empirically-based ones

(Angioni, NF, 2022; Luda di Cortemiglia, NF, 2020; Abbate, PoP, 2024; Slendebroek, PoP, 2023; Garcia, NF, 2023)

- Empirically-based models use energy confinement time (τ_E) scaling laws
- An arbitrary scalar multiple (H_{98}) is often applied to adjust this performance
- $P_M^{-0.69}$ does not capture critical gradient effects from turbulence
- τ_E does not separate core and pedestal dependencies
- τ_E does not capture nonmonotonic pedestal dependencies



Predicted versus measured stored energy



IPB98(y,2) scaling

$$\tau_H = 0.145 \frac{I_M^{0.93} R_0^{1.39} a^{0.58} \kappa^{0.78} \bar{n}_{20}^{0.41} B_0^{0.15} A^{0.19}}{P_M^{0.69}}$$

(Ch2 ITER Physics Basis)

$$\tau_E = H_{98} \times \tau_H$$

Some parameters cannot change after the tokamak design is fixed

Operation stage



What is the best way to operate the device we have?

Design stage

What is the best tokamak design for my needs?

Operation optimization

What is the best way to operate each potential design?

Operation stage parameters
Impurity mix
Fueling
Plasma shape*

Design stage parameters
Major radius (R)
Minor radius (a)
PF coil locations
Vacuum vessel shape

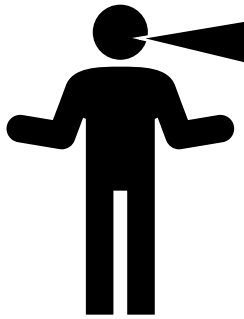
*Possible ranges determined by design stage decisions

Tokamak cartoon generated using Google AI studio

Some parameters cannot change after the tokamak design is fixed

Operation stage





What is the best way to operate the device we have?

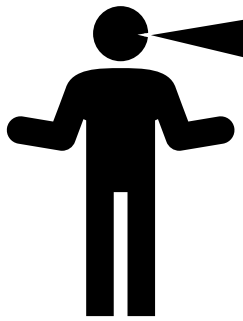
While performance predictions of operation for a given design are now regularly performed with physics-based models, initial design typically leverages empirically-based models

Sorbom, FED, 2015
Costley, NF, 2015
Zohm, JFE, 2019
Creely, PoP, 2020
Kembleton, FES, 2022
Cai, FST, 2022
Weisberg, FST, 2023
Wu, FST, 2025
Angioni, NF, 2026
Wilson, NF, 2026
Hillesheim, JPP, 2026

Operation optimization

What is the best way to operate each potential design?

Design stage



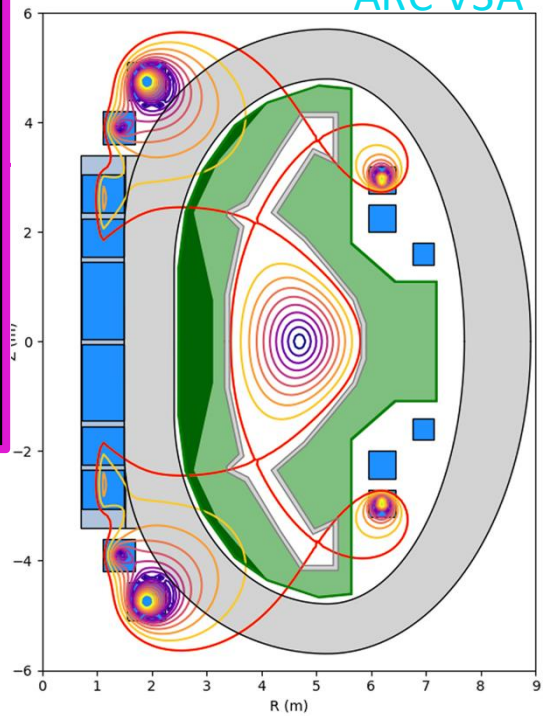


What is the best tokamak design for my needs?

Tokamak cartoon generated using Google AI studio

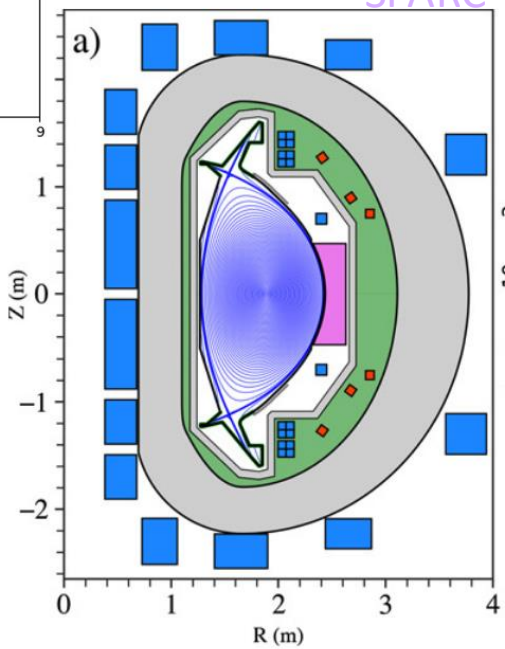
Here we demonstrate a workflow using steady state physics-based models for core transport, pedestal pressure, and detachment access to perform both operational and full design optimization for high field tokamaks.

ARC V3A



Hillesheim, JPP, 2026

SPARC

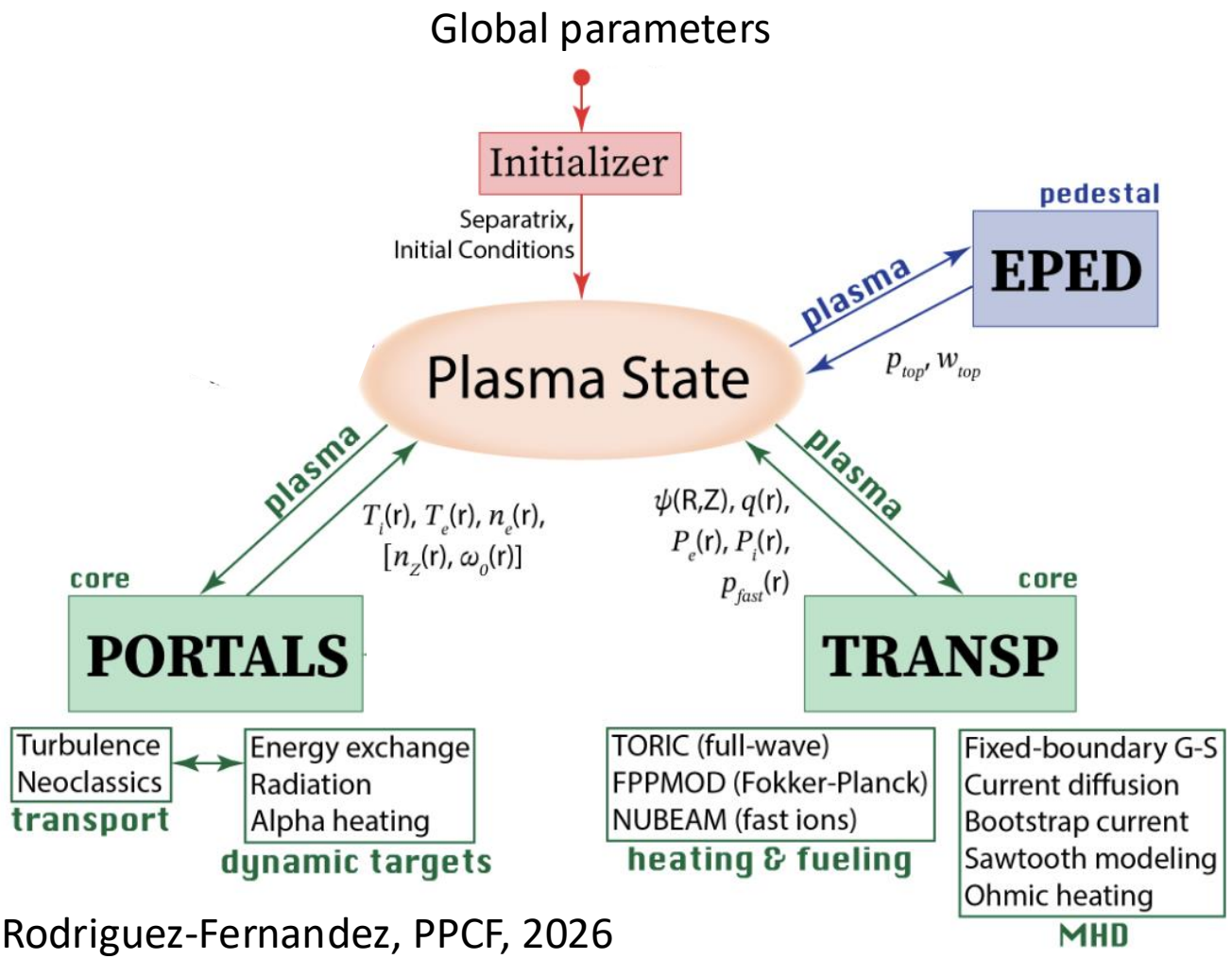


Rodriguez-Fernandez, NF, 2022

Talk plan

1. Operational optimization (max P_{fus}) of ARC-like device
2. Operational optimization (max Q) of SPARC PRD
3. Design optimization

MAESTRO is used for performance predictions



Rodriguez-Fernandez, PPCF, 2026

- Steady state integrated modeling
- Control of $n_{e,ped}$ is assumed
- MXH parameterization used as EPED input (Arbon, PPCF, 2020; Snyder, NF, 2011; modification by M. Anastopoulos Tzanis)
- PORTALS-TGLF SAT2 (Staebler, NF, 2021)
- Flat Z_{eff} profiles assumed (Muraca, PPCF, 2026)
- Radiation calculated with fit to ADAS database
- Pulse duration (τ_{pulse}) calculations using model in Barr, NF, 2018 made with CFSPOPCON

MAESTRO is used for performance predictions

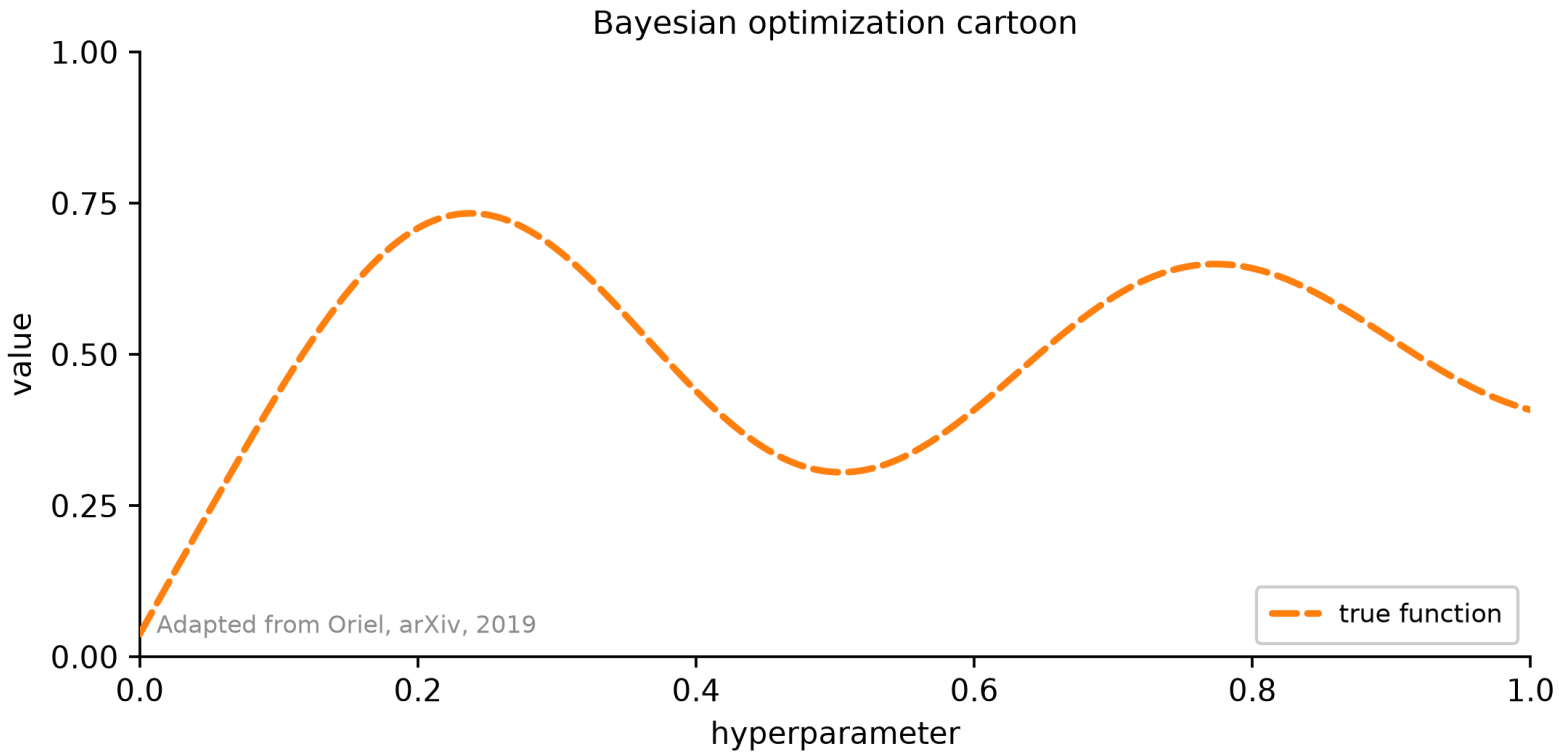
MAESTRO is black box in optimization

~100 CPU hours per simulation

- Steady state integrated modeling
- Control of $n_{e,ped}$ is assumed
- MXH parameterization used as EPED input (Arbon, PPCF, 2020; Snyder, NF, 2011; modification by M. Anastopoulos Tzanis)
- PORTALS-TGLF SAT2 (Staebler, NF, 2021)
- Flat Z_{eff} profiles assumed
- Radiation calculated with fit to ADAS database
- Pulse duration (τ_{pulse}) calculations using model in Barr, NF, 2018 made with CFSPOPCON

Bayesian optimization (BO) used to efficiently search input parameters

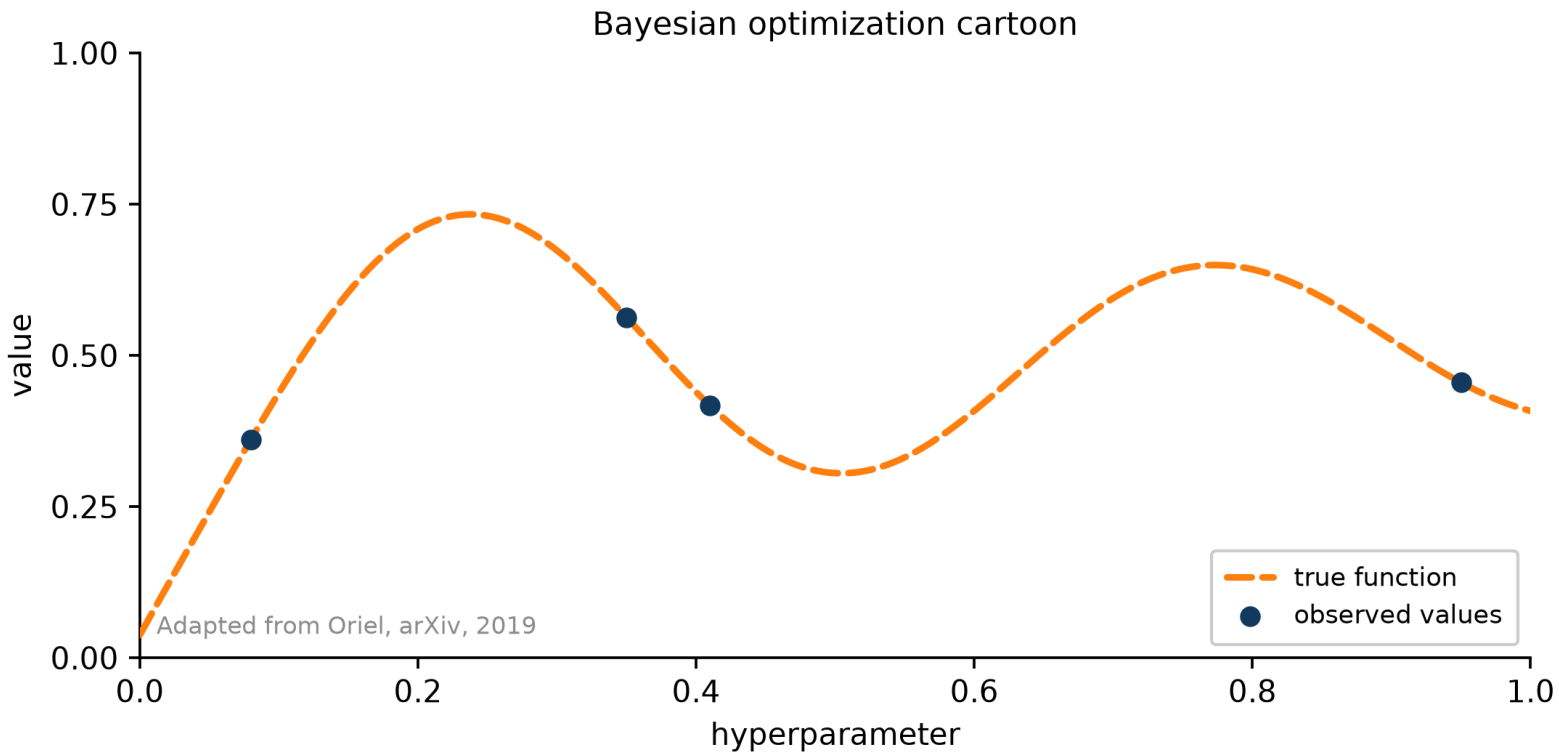
BO Steps



Bayesian optimization (BO) used to efficiently search input parameters

BO Steps

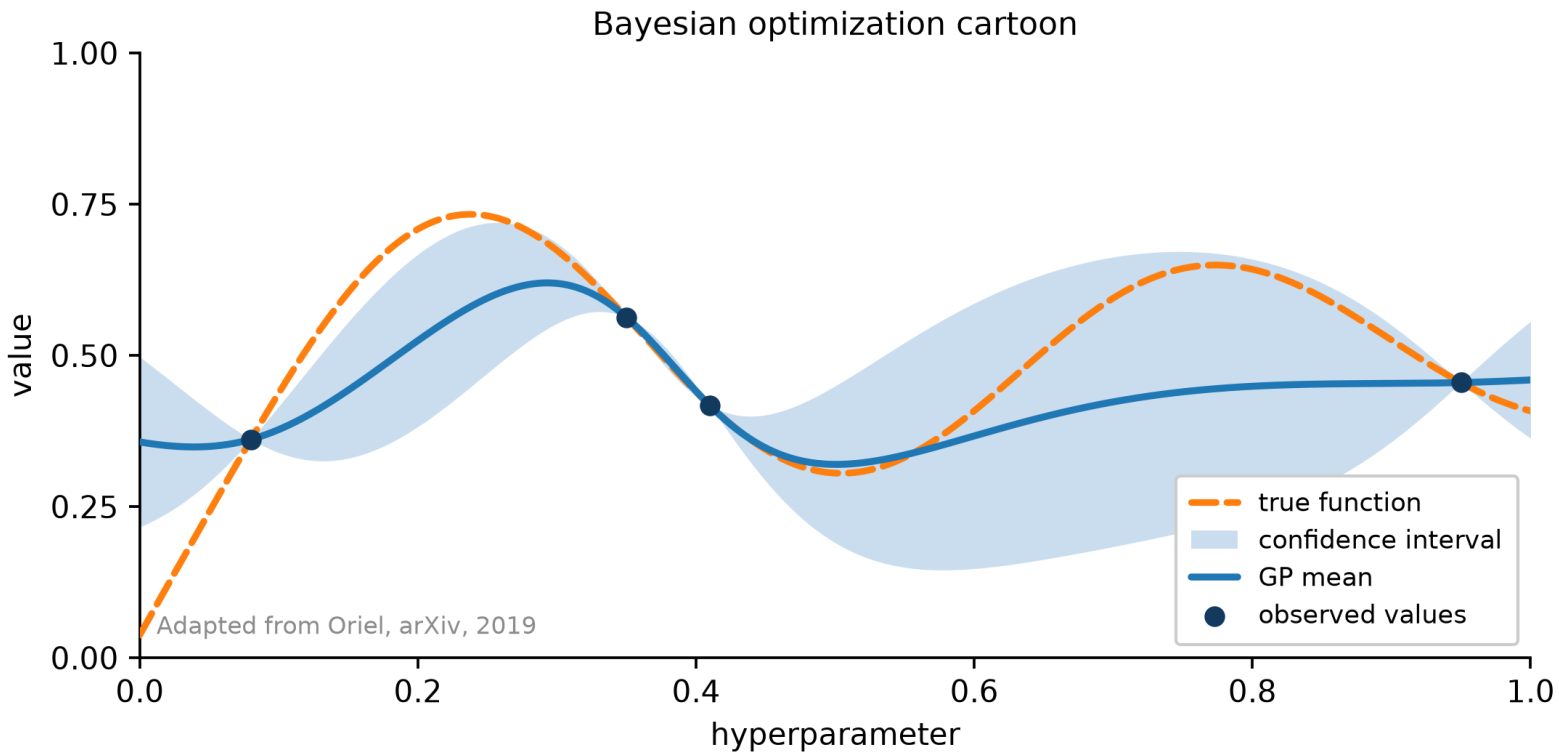
1. Acquire training data



Bayesian optimization (BO) used to efficiently search input parameters

BO Steps

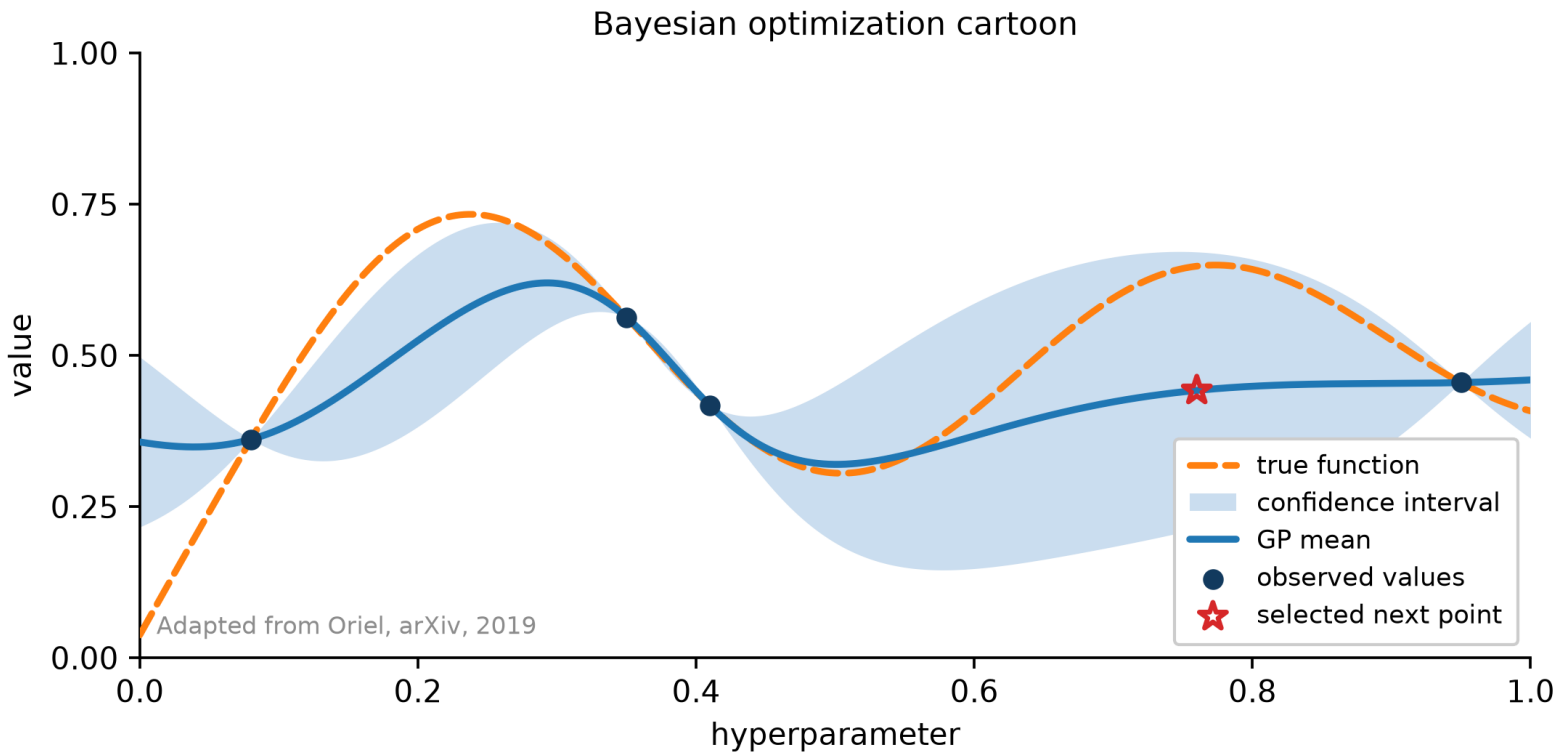
1. Acquire training data
2. Fit surrogate



Bayesian optimization (BO) used to efficiently search input parameters

BO Steps

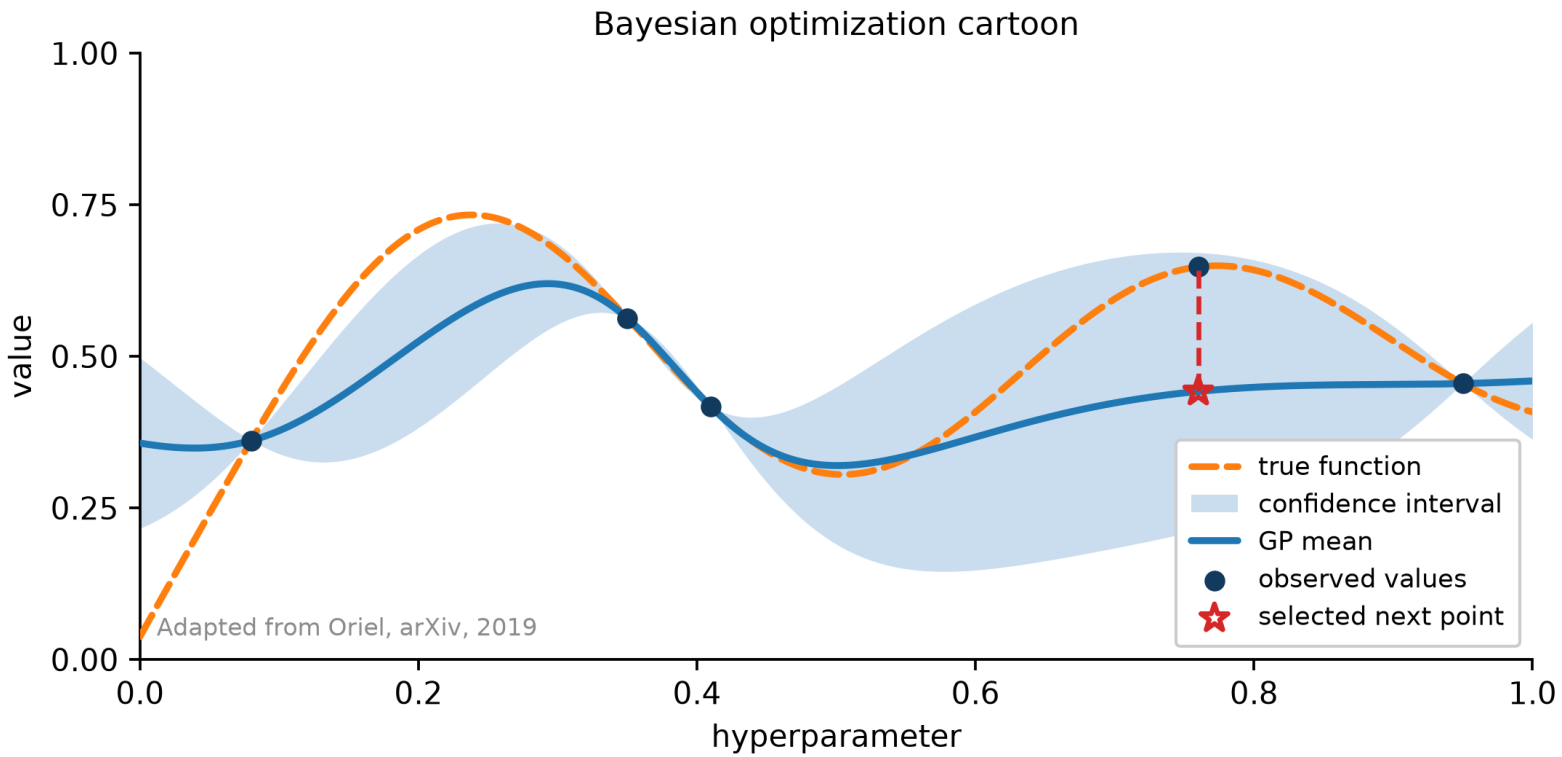
1. Acquire training data
2. Fit surrogate
3. Evaluate acquisition function to determine next point(s) to evaluate



Bayesian optimization (BO) used to efficiently search input parameters

BO Steps

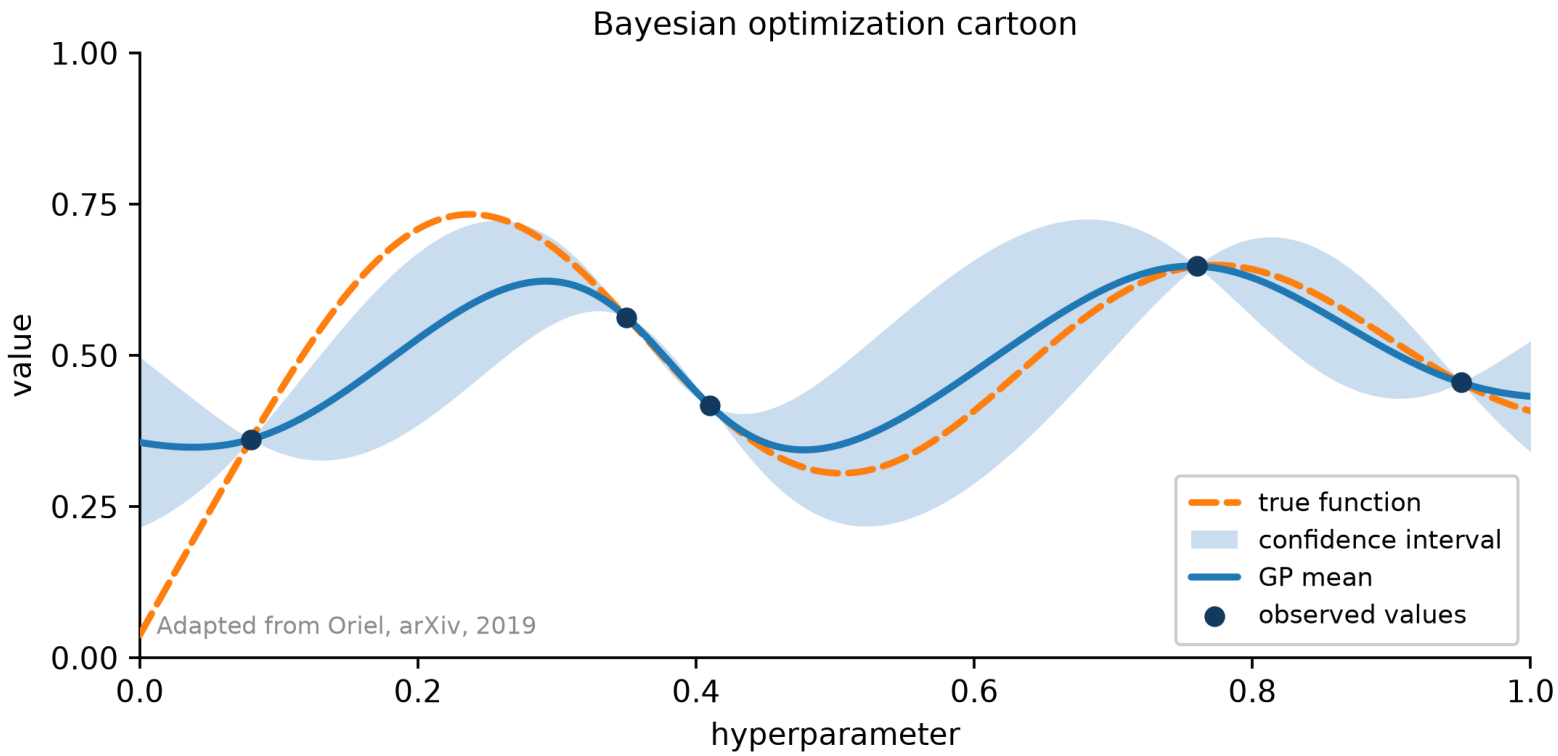
1. Acquire training data
2. Fit surrogate
3. Evaluate acquisition function to determine next point(s) to evaluate
4. Repeat



Bayesian optimization (BO) used to efficiently search input parameters

BO Steps

1. Acquire training data
2. Fit surrogate
3. Evaluate acquisition function to determine next point(s) to evaluate
4. Repeat



Reference tutorial: Frazier, arXiv, 2018

Operational optimization enables increase in P_{fus} for an ARC-like device

ARC V3A Optimization Problem

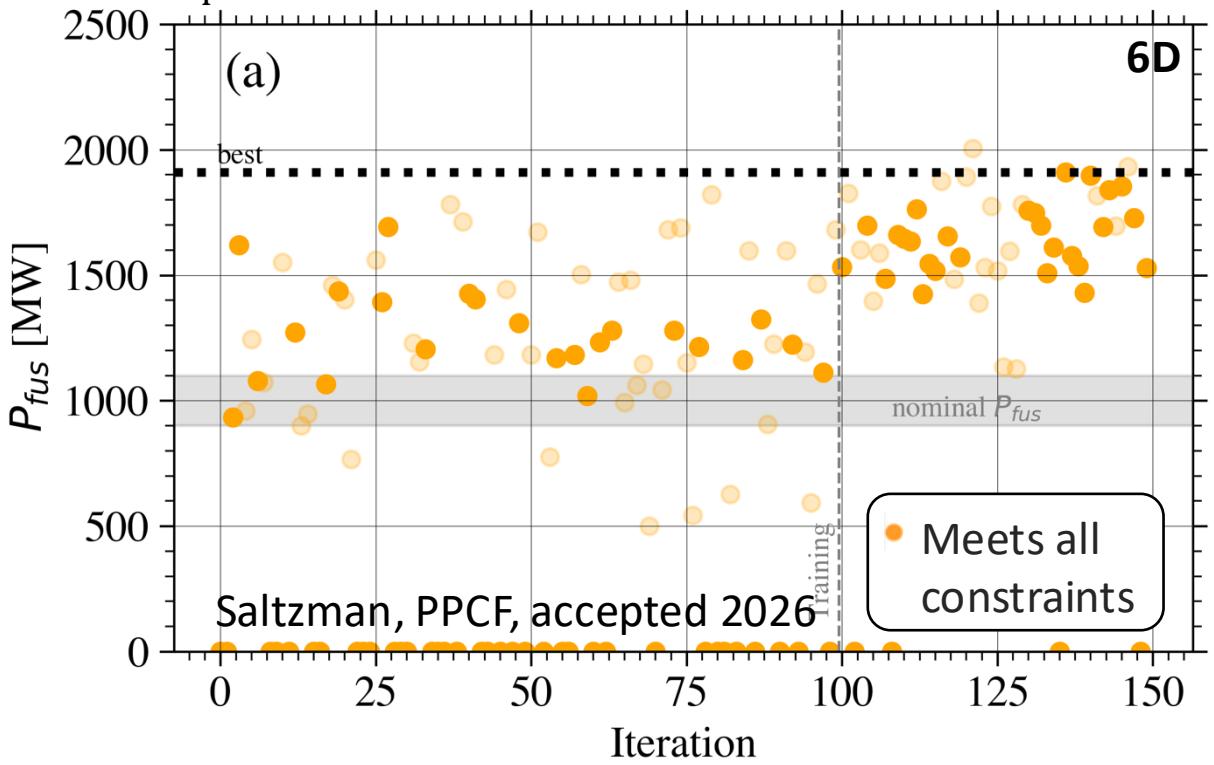
$$\max_{(Z_{eff}, f_{main}, n_{e,ped}, \kappa, \delta, \zeta)} P_{fus}$$

$$\text{s.t.} \quad \langle n_e \rangle < 0.9\, n_G$$

$$P_{sol} > P_{LH}$$

- ~65% increase in P_{fus} for extended range of κ and squareness variation
- ~30% increase in P_{fus} possible for fixed κ
- Higher Z_{eff} & large positive squareness preferred
- τ_{pulse} ↑ due to $\langle T_e \rangle$ ↑, although Z_{eff} is higher

Variable	Nominal	6D
Z_{eff}	1.5	2.1
f_{main}	0.85	0.88
κ	1.77	1.99
δ	0.49	0.60
ζ	0	0.17
$n_{e,ped}[\times 10^{20}/m^3]$	2.10	2.18
$P_{fus}[MW]$	1140	1910
$\tau_{flattop}$ [s]	1021	1071



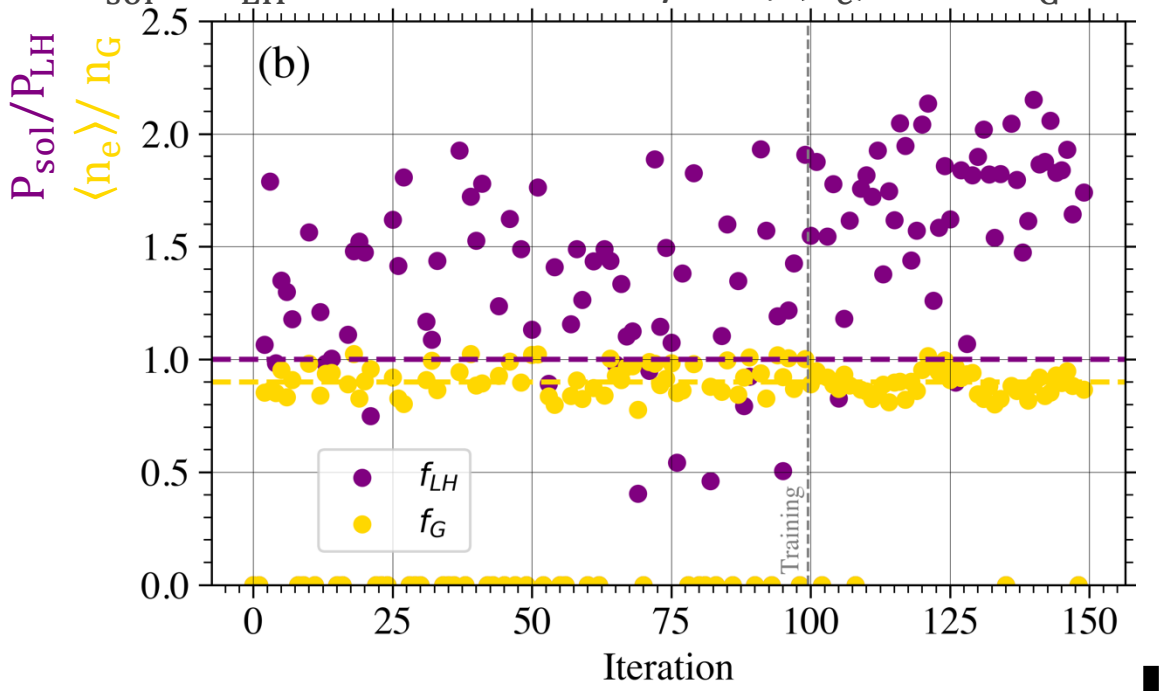
Operational optimization enables increase in P_{fus} for an ARC-like device

ARC V3A Optimization Problem

$$\max_{(Z_{eff}, f_{main}, n_{e,ped}, \kappa, \delta, \zeta)} P_{fus}$$
$$\text{s.t.} \quad \langle n_e \rangle < 0.9\, n_G$$
$$P_{sol} > P_{LH}$$

- ~65% increase in P_{fus} for extended range of κ and squareness variation
- ~30% increase in P_{fus} possible for fixed κ
- Higher Z_{eff} & large positive squareness preferred
- τ_{pulse} ↑ due to $\langle T_e \rangle$ ↑, although Z_{eff} is higher
- $P_{sol} > P_{LH}$ constraint is readily met, $\langle n_e \rangle < 0.9\, n_G$ constraint is limiting

Variable	Nominal	6D
Z_{eff}	1.5	2.1
f_{main}	0.85	0.88
κ	1.77	1.99
δ	0.49	0.60
ζ	0	0.17
$n_{e,ped}[\times 10^{20}/m^3]$	2.10	2.18
$P_{fus}[MW]$	1140	1910
$\tau_{flattop}$ [s]	1021	1071



Saltzman, PPCF, accepted 2026

Despite tradeoffs, stronger shaping, including positive squareness is beneficial

ARC-like

	Volume	ITG Stability	Peeling branch pressure	Density of ballooning limited
κ	↑	↑		
δ	↓	↓		
ζ				

- Elongation is favorable considering impacts on volume and ITG stability, triangularity is not (Belli, PoP, 2008)

Despite tradeoffs, stronger shaping, including positive squareness is beneficial

ARC-like

	Volume	ITG Stability	Peeling branch pressure	Density of ballooning limited
κ	↑	↑	↓	↑
δ	↓	↓		
ζ				

- Elongation is favorable considering impacts on volume and ITG stability, triangularity is not (Belli, PoP, 2008)
- Higher elongation greatly increases the density at which ballooning modes limit the pedestal (Kim, PoP, 2022)

Despite tradeoffs, stronger shaping, including positive squareness is beneficial

ARC-like

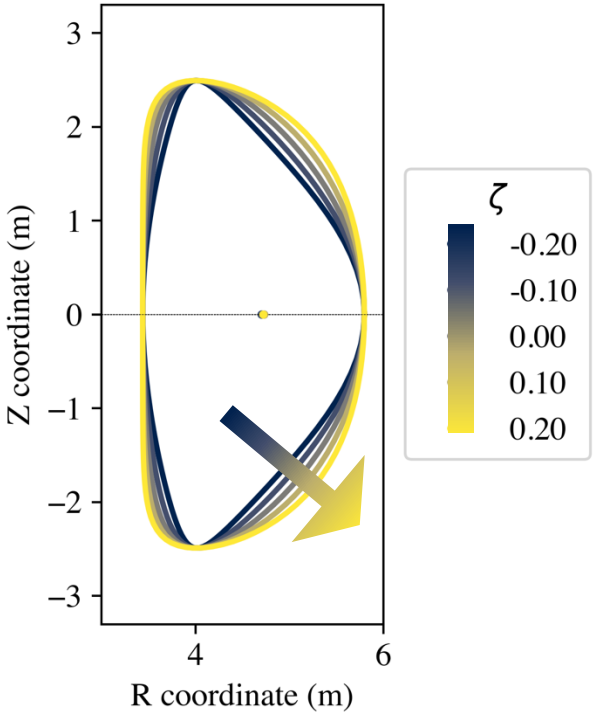
	Volume	ITG Stability	Peeling branch pressure	Density of ballooning limited
κ	↑	↑	↓	↑
δ	↓	↓	↑	↓
ζ				

- Elongation is favorable considering impacts on volume and ITG stability, triangularity is not (Belli, PoP, 2008)
- Higher elongation greatly increases the density at which ballooning modes limit the pedestal (Kim, PoP, 2022)
- Higher triangularity greatly increases the pressure on the peeling branch (Kim, PoP, 2022)

Despite tradeoffs, stronger shaping, including positive squareness is beneficial

ARC-like

	Volume	ITG Stability	Peeling branch pressure	Density of ballooning limited
κ	↑	↑	↓	↑
δ	↓	↓	↑	↓
ζ	↑			

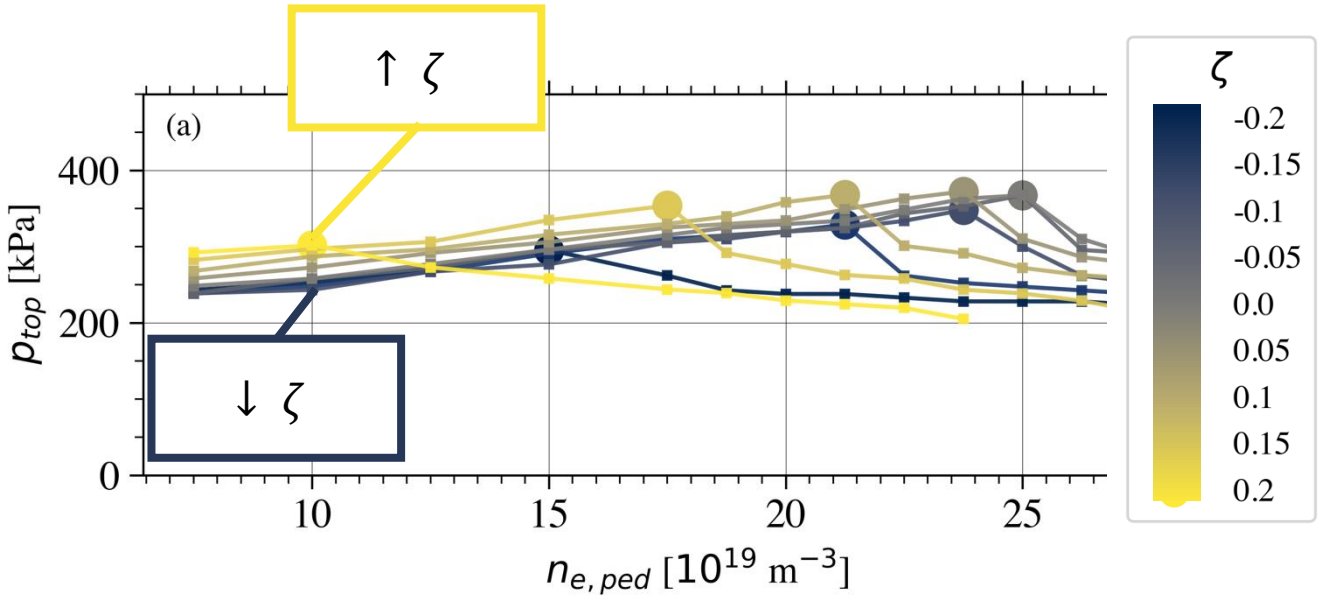


- Elongation is favorable considering impacts on volume and ITG stability, triangularity is not (Belli, PoP, 2008)
- Higher elongation greatly increases the density at which ballooning modes limit the pedestal (Snyder, PPCF, 2024)
- Higher triangularity greatly increases the pressure on the peeling branch (Snyder, PPCF, 2024)
- Higher squareness increases plasma volume

Despite tradeoffs, stronger shaping, including positive squareness is beneficial

ARC-like

	Volume	ITG Stability	Peeling branch pressure	Density of ballooning limited
κ	↑	↑	↓	↑
δ	↓	↓	↑	↓
ζ	↑	∅	↑	

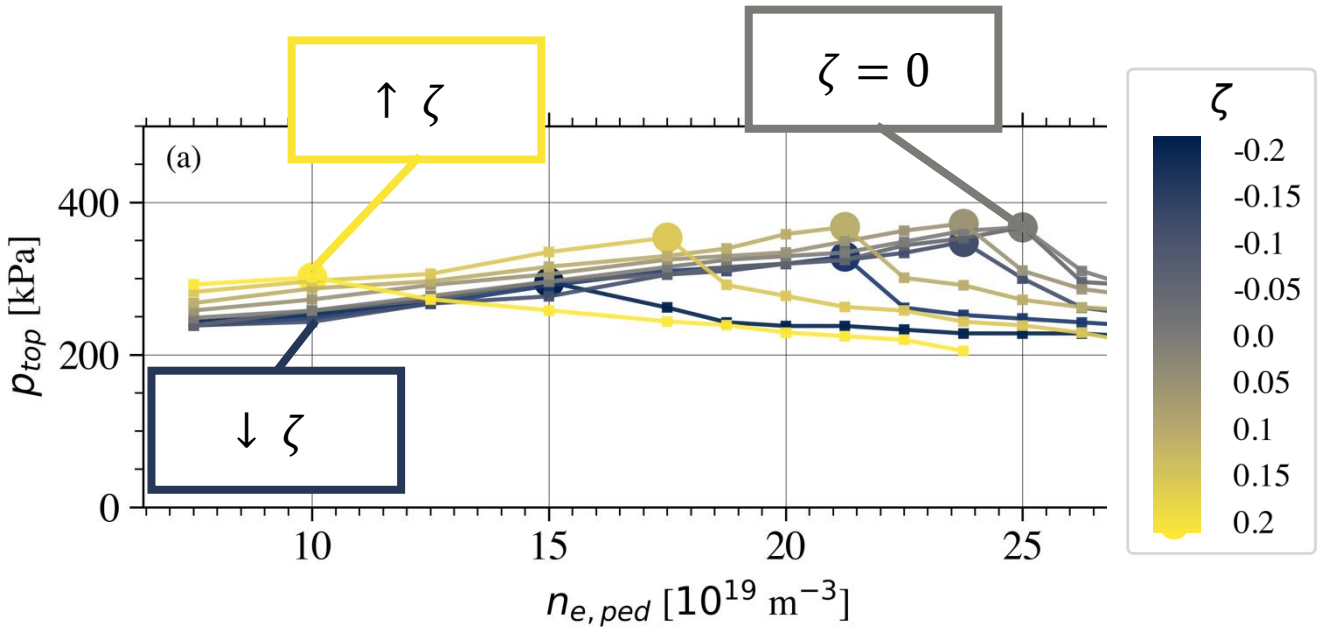


- Elongation is favorable considering impacts on volume and ITG stability, triangularity is not (Belli, PoP, 2008)
- Higher elongation greatly increases the density at which ballooning modes limit the pedestal (Kim, PoP, 2022)
- Higher triangularity greatly increases the pressure on the peeling branch (Kim, PoP, 2022)
- Higher squareness increases plasma volume
- Higher squareness also increases the pressure on the peeling branch

Despite tradeoffs, stronger shaping, including positive squareness is beneficial

ARC-like

	Volume	ITG Stability	Peeling branch pressure	Density of ballooning limited
κ	↑	↑	↓	↑
δ	↓	↓	↑	↓
ζ	↑	∅	↑	$\lvert\zeta\rvert \propto \downarrow$

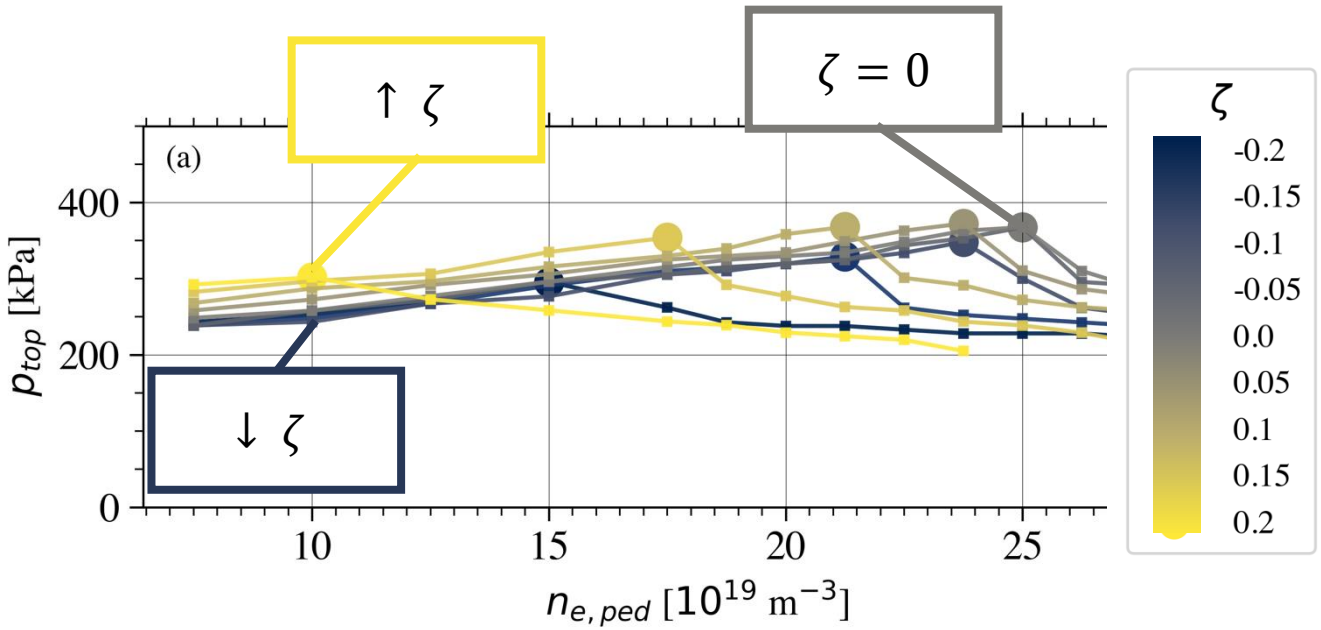


- Elongation is favorable considering impacts on volume and ITG stability, triangularity is not (Belli, PoP, 2008)
- Higher elongation greatly increases the density at which ballooning modes limit the pedestal (Kim, PoP, 2022)
- Higher triangularity greatly increases the pressure on the peeling branch (Kim, PoP, 2022)
- Higher squareness increases plasma volume
- Higher squareness also increases the pressure on the peeling branch
- The density at which ballooning modes limit the pedestal is highest for $\zeta = 0$

Despite tradeoffs, stronger shaping, including positive squareness is beneficial

ARC-like

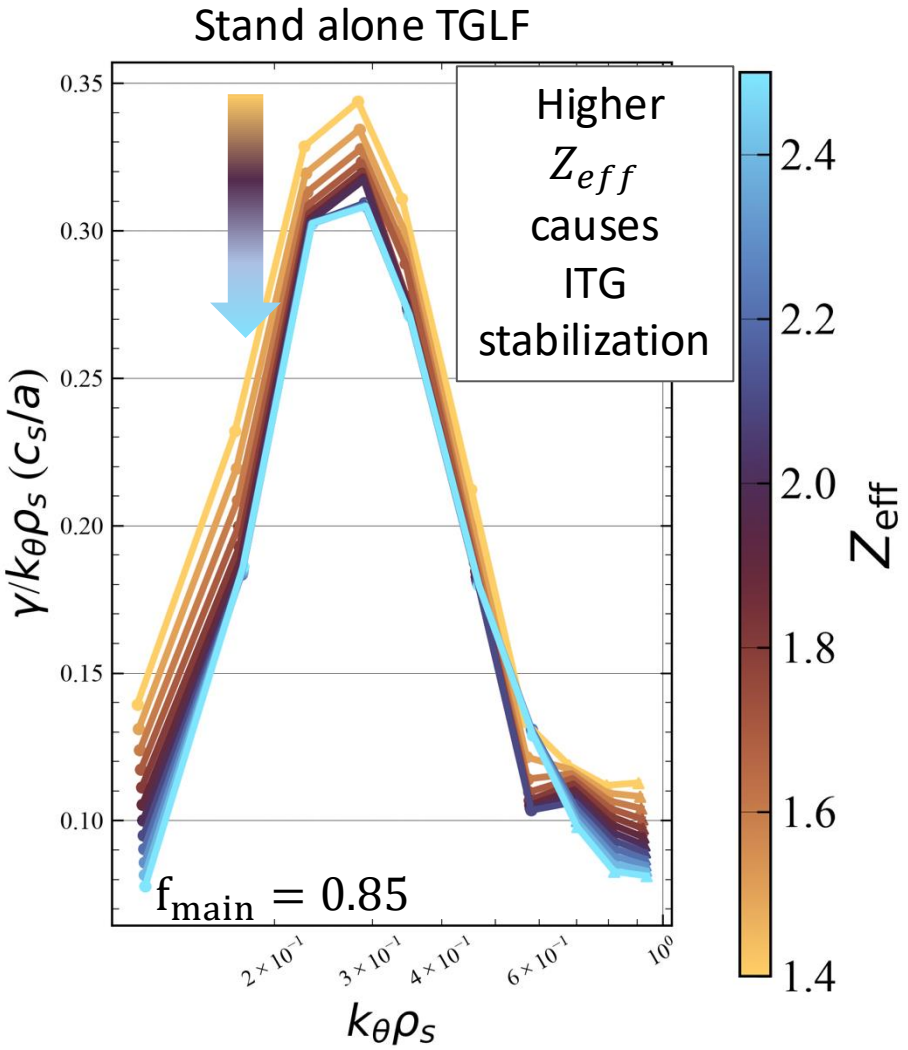
Optimization with varying squareness allows a 25% greater increase in P_{fus} than when it is not varied.



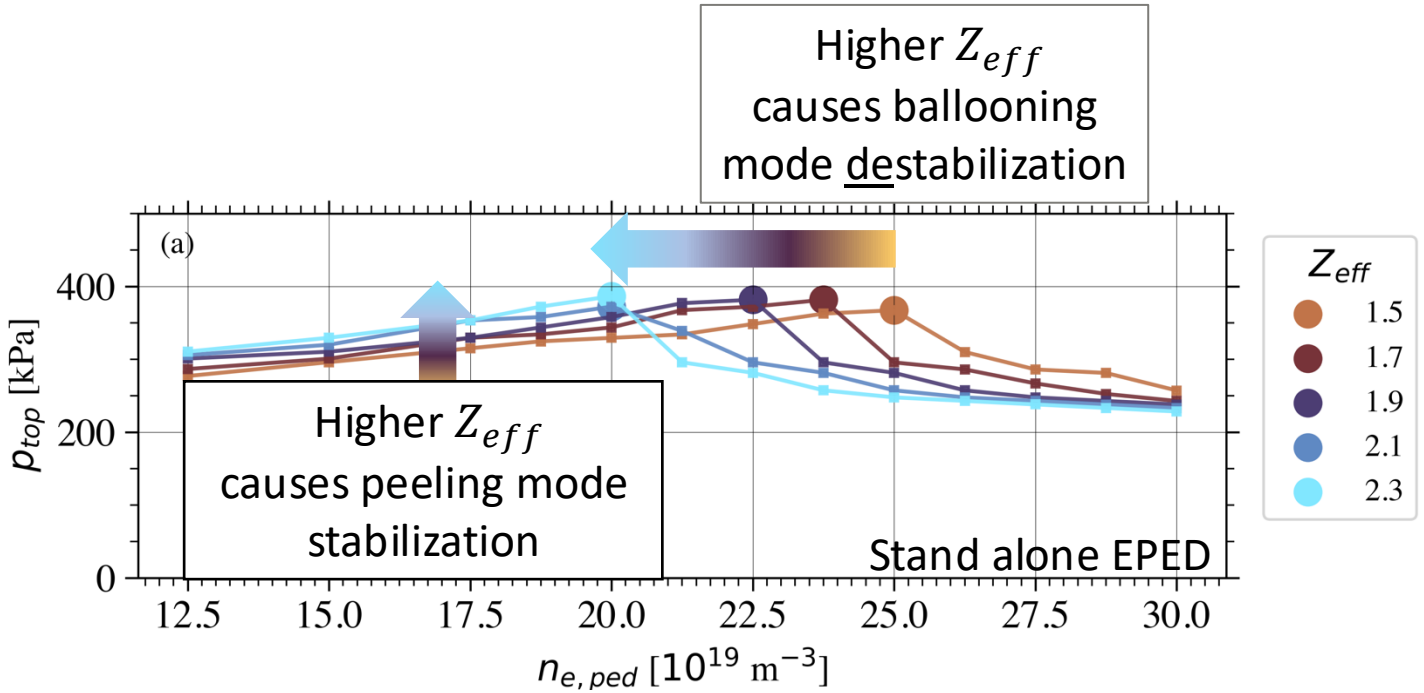
- Elongation is favorable considering impacts on volume and ITG stability, triangularity is not (Belli, PoP, 2008)
- Higher elongation greatly increases the density at which ballooning modes limit the pedestal (Kim, PoP, 2022)
- Higher triangularity greatly increases the pressure on the peeling branch (Kim, PoP, 2022)
- Higher squareness increases plasma volume
- Higher squareness also increases the pressure on the peeling branch
- The density at which ballooning modes limit the pedestal is highest for $\zeta = 0$

More impurities result in ITG (core) and peeling mode (pedestal) stabilization

ARC-like



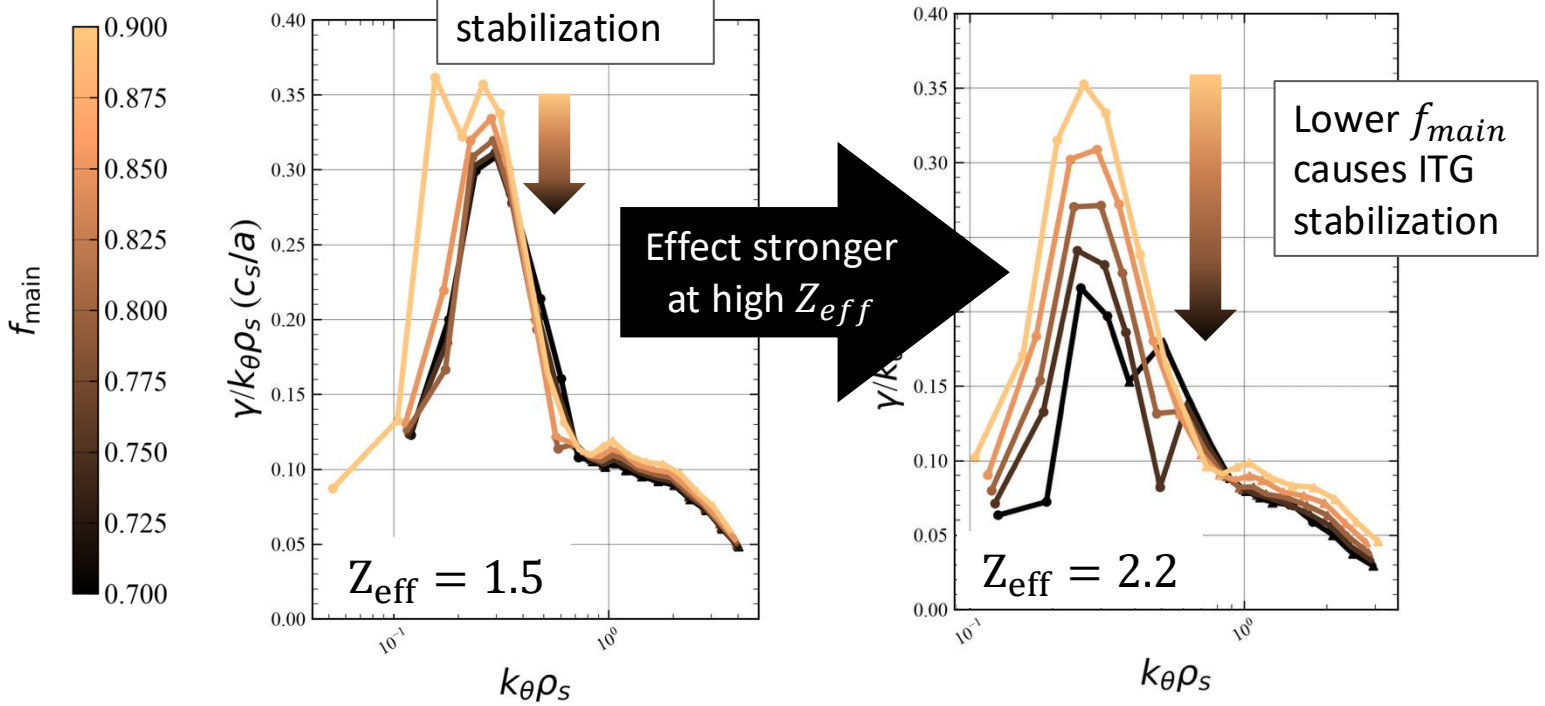
- Z_{eff} drives both ITG and peeling mode stabilization but decreases the density at which p_{top} is highest (consistent with Snyder, NF, 2019)



More impurities result in ITG (core) and peeling mode (pedestal) stabilization

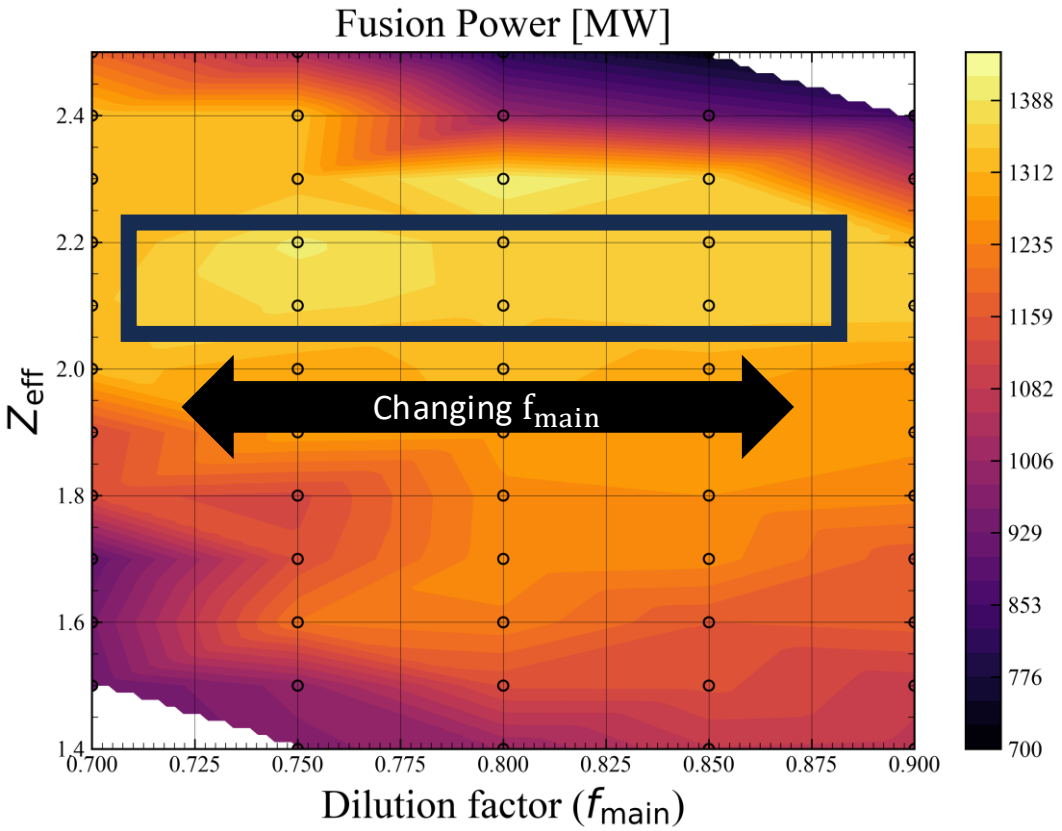
ARC-like

- Z_{eff} drives both ITG and peeling mode stabilization but decreases the density at which p_{top} is highest (consistent with Snyder, NF, 2019)
- Z_{eff} and f_{main} impacts on turbulence are coupled (consistent with Rodriguez-Fernandez, APS DPP, 2025)



More impurities result in ITG (core) and peeling mode (pedestal) stabilization

ARC-like



- Z_{eff} drives both ITG and peeling mode stabilization but decreases the density at which p_{top} is highest (consistent with Snyder, NF, 2019)
- Z_{eff} and f_{main} impacts on turbulence are coupled (consistent with Rodriguez-Fernandez, APS DPP, 2025)
- P_{fus} is nearly constant with f_{main} because ITG stabilization and dilution cancel out

Empirical modeling would not be able to capture beneficial impact of impurities

ARC-like

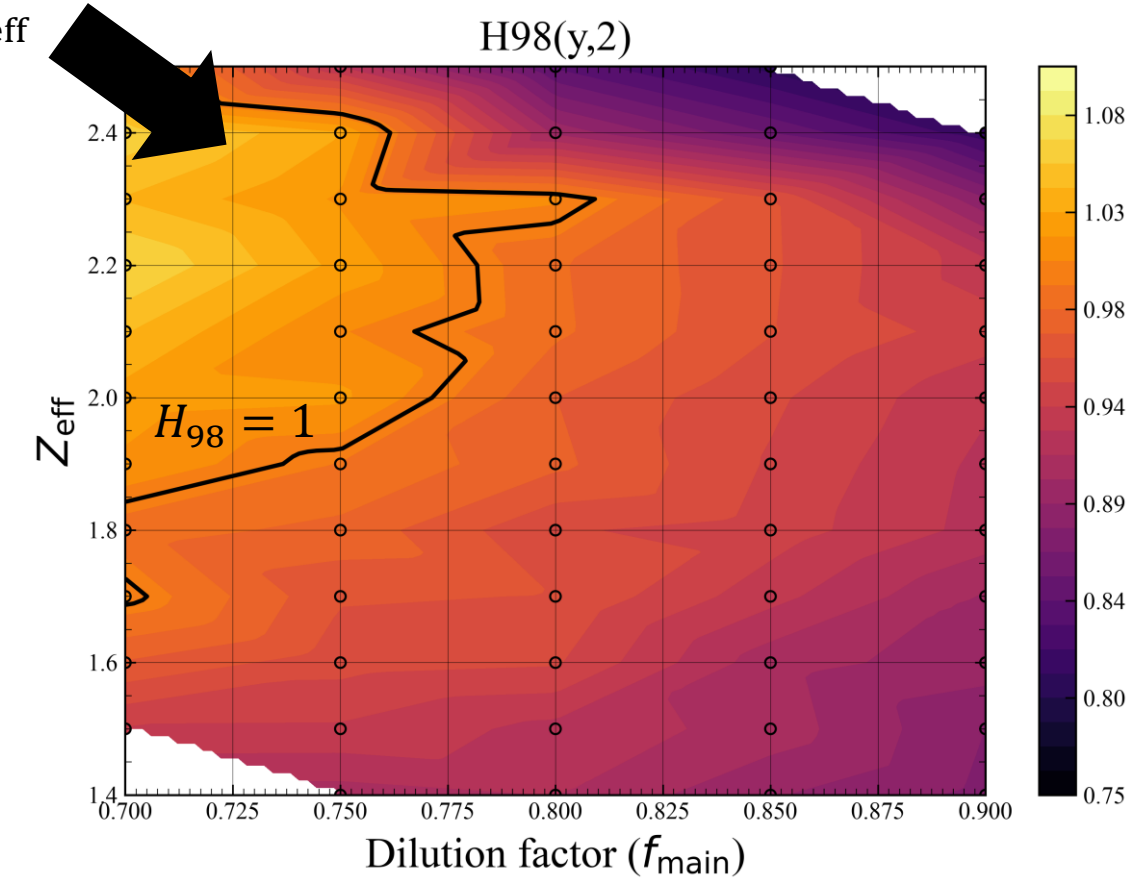
- Here we calculate the value of H_{98} required to get the simulation τ_E
- τ_H strongly underpredicts benefit of low f_{main} and high Z_{eff}

ITB98(y,2) scaling

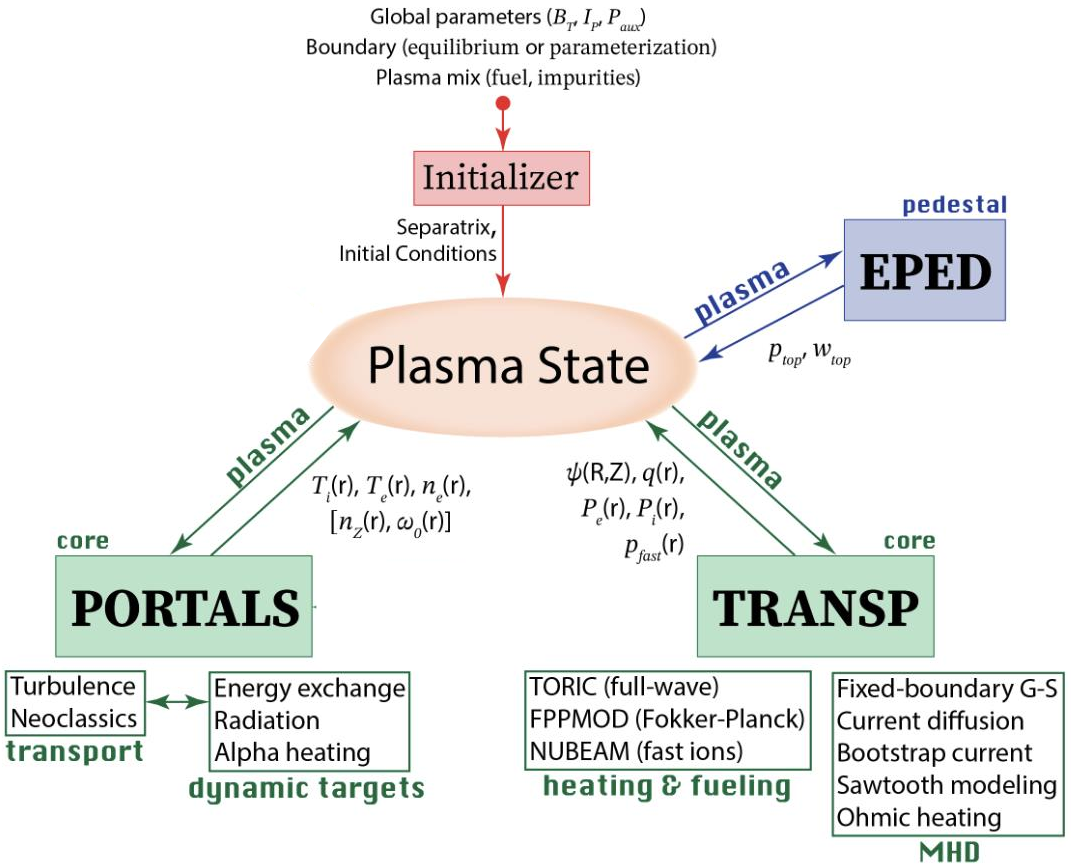
$$\tau_H = 0.145 \frac{I_M^{0.93} R_0^{1.39} a^{0.58} \kappa^{0.78} \bar{n}_{20}^{0.41} B_0^{0.15} A^{0.19}}{P_M^{0.69}}$$

(Ch2 ITER Physics Basis)

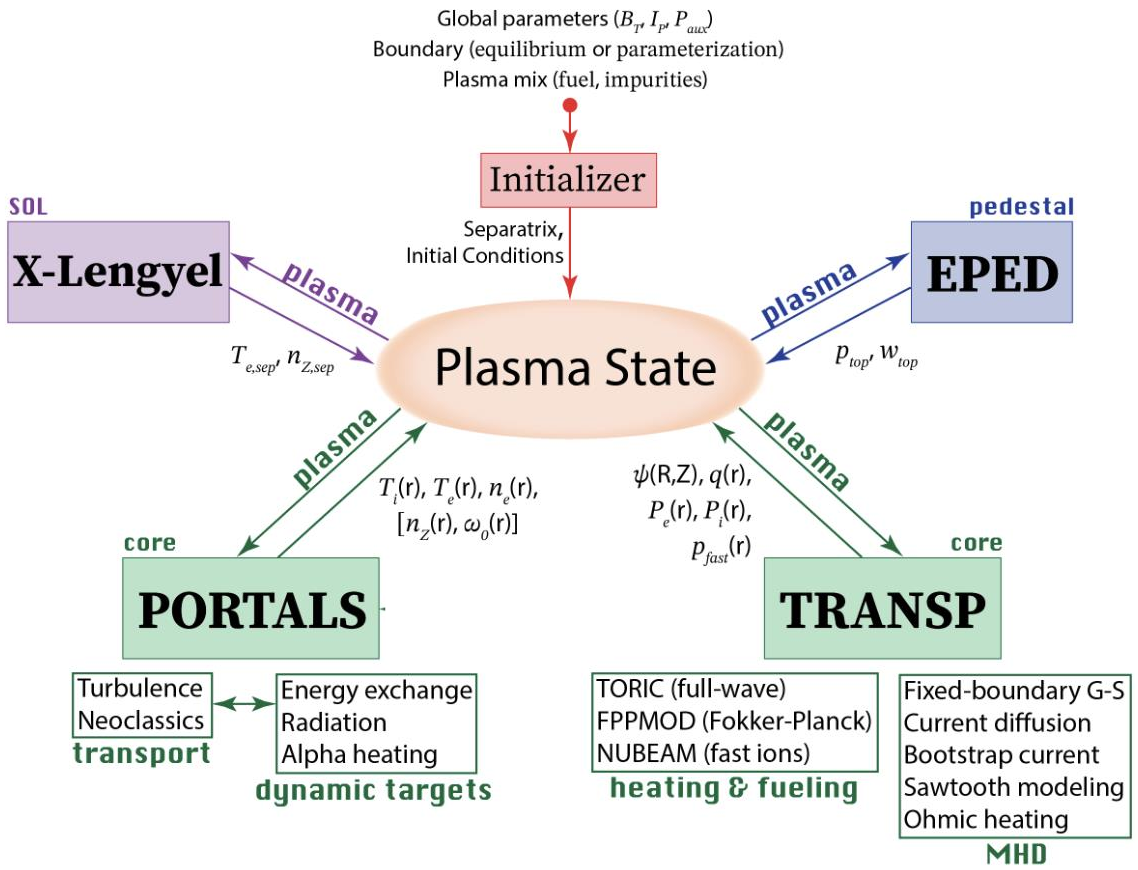
$$\tau_E = H_{98} \times \tau_H$$



Core-edge integration tested with Extended Lengyel (XLGL) model coupling

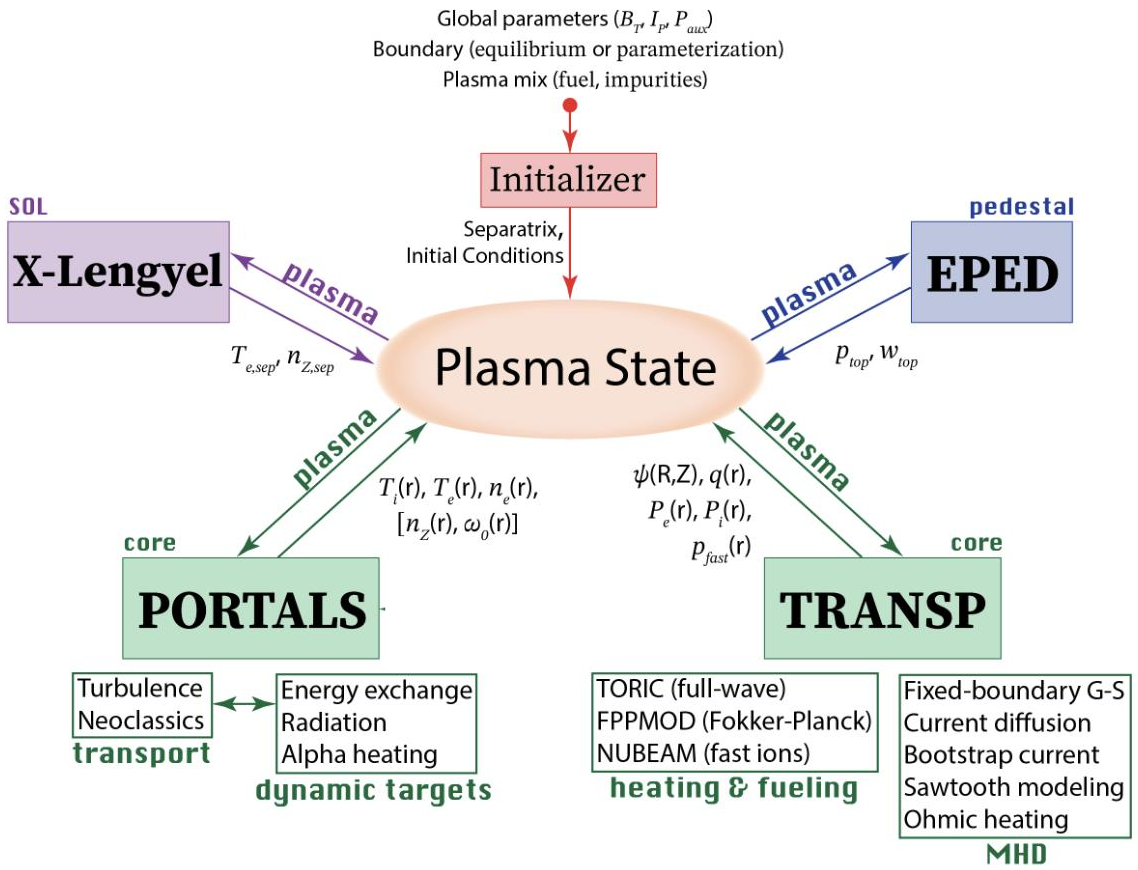


Core-edge integration tested with Extended Lengyel (XLGL) model coupling



- We use MAESTRO's coupling with the Extended Lengyel Model (Body, NF, 2025) that models detachment access

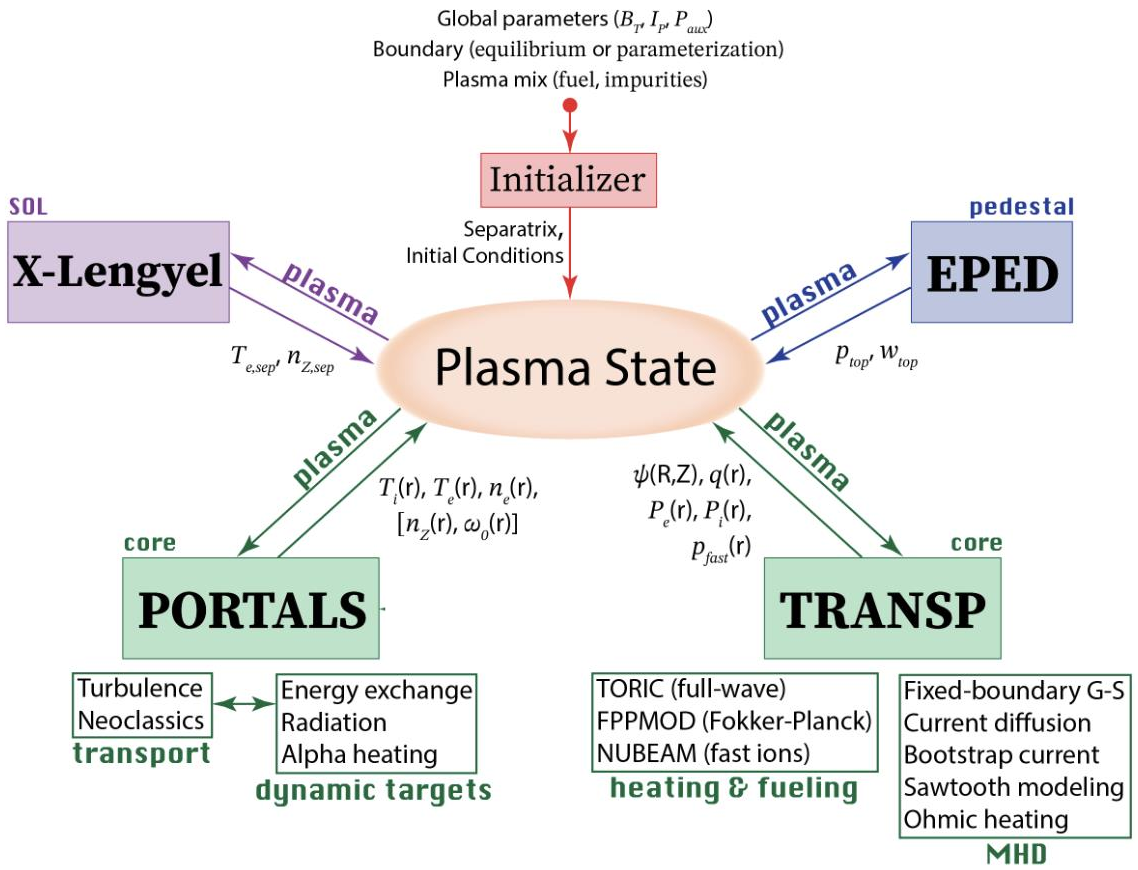
Core-edge integration tested with Extended Lengyel (XLGL) model coupling



- We use MAESTRO's coupling with the Extended Lengyel Model (Body, NF, 2025) that models detachment access
- Instead of Z_{eff} and f_{main}, lithium is now varied in optimization

	Concentration ($f_{Li} = {}^{n_x}/_{n_e}$)
Li	Controlled by optimization

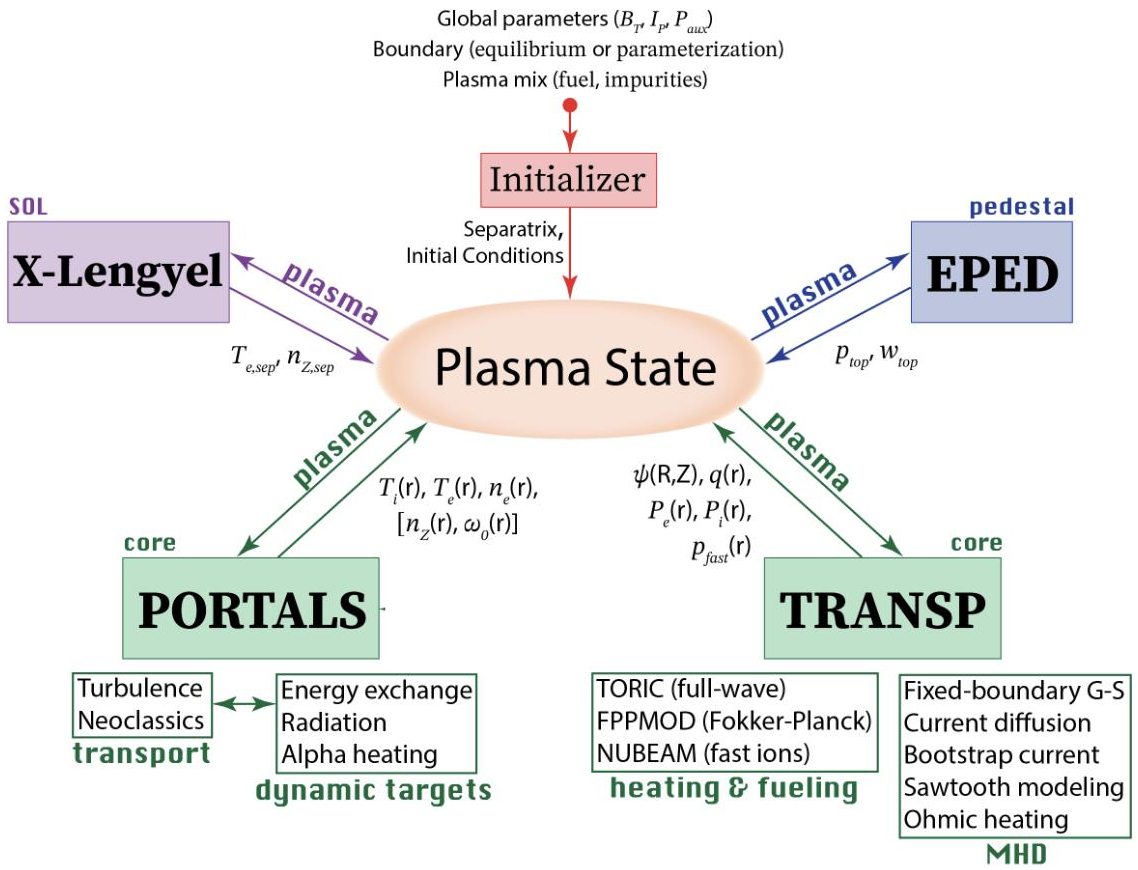
Core-edge integration tested with Extended Lengyel (XLGL) model coupling



- We use MAESTRO's coupling with the Extended Lengyel Model (Body, NF, 2025) that models detachment access
- Instead of Z_{eff} and f_{main}, lithium is now varied in optimization
- Fixed impurities include tungsten, hydrogen, and helium ash

	Concentration ($f_{Li} = {}^{n_x}/_{n_e}$)
Li	Controlled by optimization
W	1.5×10^{-5}
H	3%, ICRH minority
He	5% ash + fast ions consistent with P_{fus}

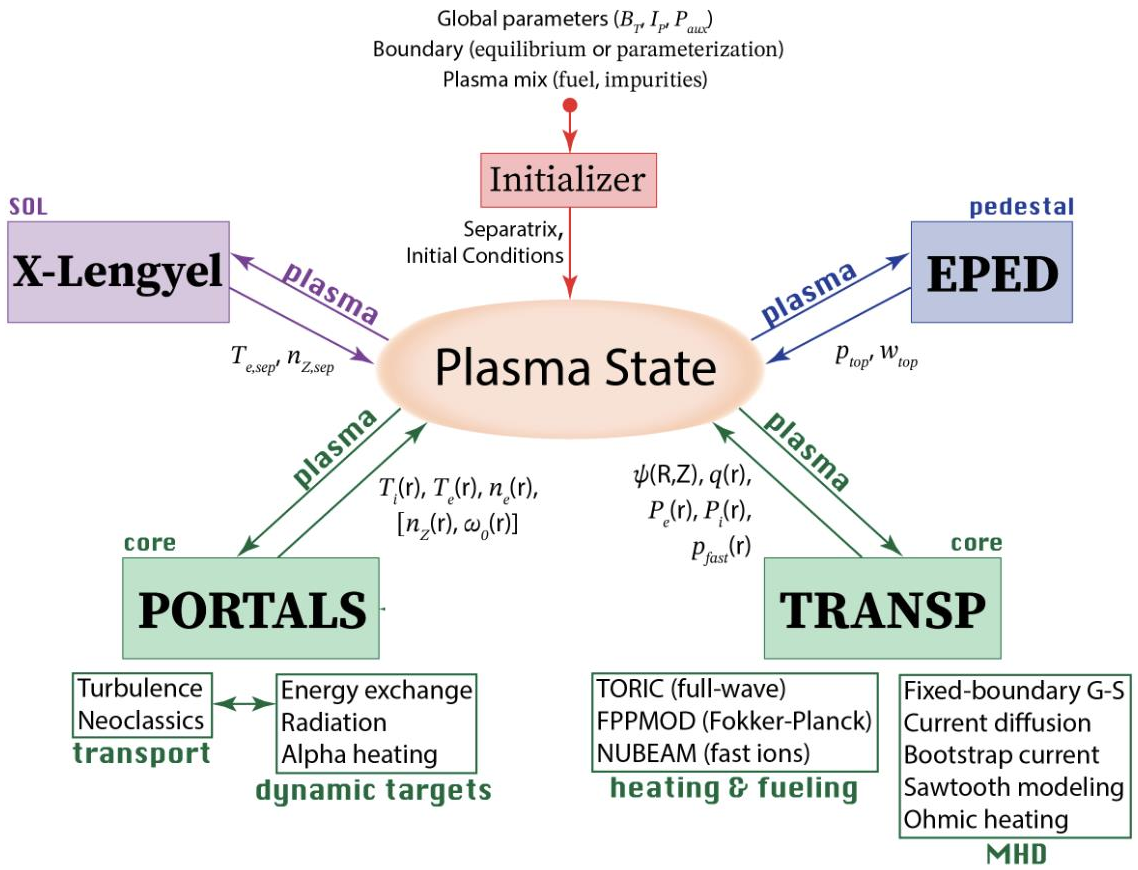
Core-edge integration tested with Extended Lengyel (XLGL) model coupling



- We use MAESTRO's coupling with the Extended Lengyel Model (Body, NF, 2025) that models detachment access
- Instead of Z_{eff} and f_{main}, lithium is now varied in optimization
- Fixed impurities include tungsten, hydrogen, and helium ash
- Amount of argon calculated consistent with detached divertor

	Concentration ($f_{Li} = {}^{n_x}/_{n_e}$)
Li	Controlled by optimization
W	1.5×10^{-5}
H	3%, ICRH minority
He	5% ash + fast ions consistent with P_{fus}
Ar	Calculated by XLGL

Core-edge integration tested with Extended Lengyel (XLGL) model coupling



- We use MAESTRO's coupling with the Extended Lengyel Model (Body, NF, 2025) that models detachment access
- Instead of Z_{eff} and f_{main}, a Z=3 lumped impurity is now varied
- Fixed impurities include tungsten, hydrogen, and helium ash
- Amount of argon calculated consistent with detached divertor

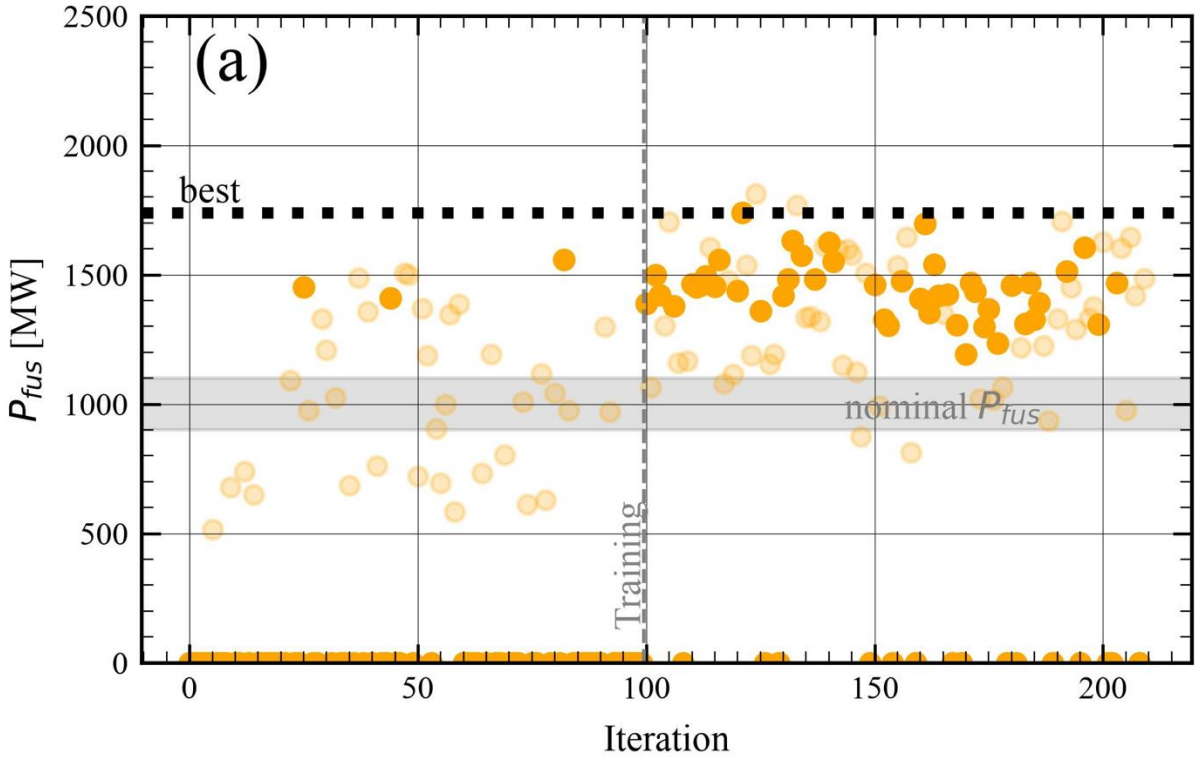
	Concentration ($f_x = {}^{n_x}/_{n_e}$)
Z = 3	Controlled by optimization
W	1.5×10^{-5}
H	3%, ICRH minority
He	5% ash + fast ions consistent with P_{fus}
Ar	Calculated by XLGL
DT	Equal, determined by quasineutrality

Comparable optimal core-edge integrated solution identified

ARC-like

$$\max \; P_{fus}(f_{Z=3}, n_{e,ped}, \kappa, \delta, \zeta)$$
$$\text{s.t.} \quad \langle n_e \rangle < 0.9\, n_G$$
$$P_{\alpha} > P_{\alpha,min}$$

- Comparable solution to original 6D optimization with 50% increase in P_{fus} (vs 65%)
- Optimal $f_{Z=3}$ = 0.3% (with argon and helium ash) results in higher Z_{eff} and lower f_{main}



Variable	Nominal	6D	With Lengyel
Z_{eff}	1.5	2.1	2.3*
f_{main}	0.85	0.88	0.78*
κ	1.77	1.99	1.93
δ	0.49	0.60	0.60
ζ	0.0	0.17	0.15
$n_{e,ped}$ $[\times 10^{20}/m^3]$	2.10	2.18	2.18
P_{fus} [MW]	1140	1910	1740

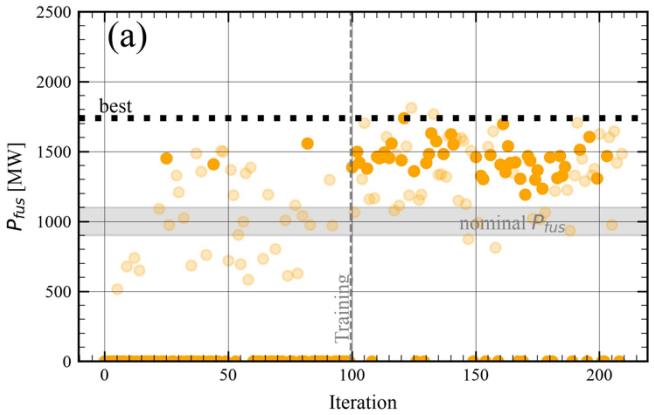
Summary: Part One

Via operational optimization, a core-edge integrated operating point with higher P_{fus} can be achieved for an ARC-like device

- Squareness is an important shaping parameter
- Impurities can benefit both core gradients and pedestal pressure

Talk plan

1. Operational optimization (max P_{fus}) of ARC-like device
2. **Operational optimization (max Q) of SPARC PRD**
3. Design optimization



At least Q>5 can be achieved with $P_{sol} > P_{LH}$

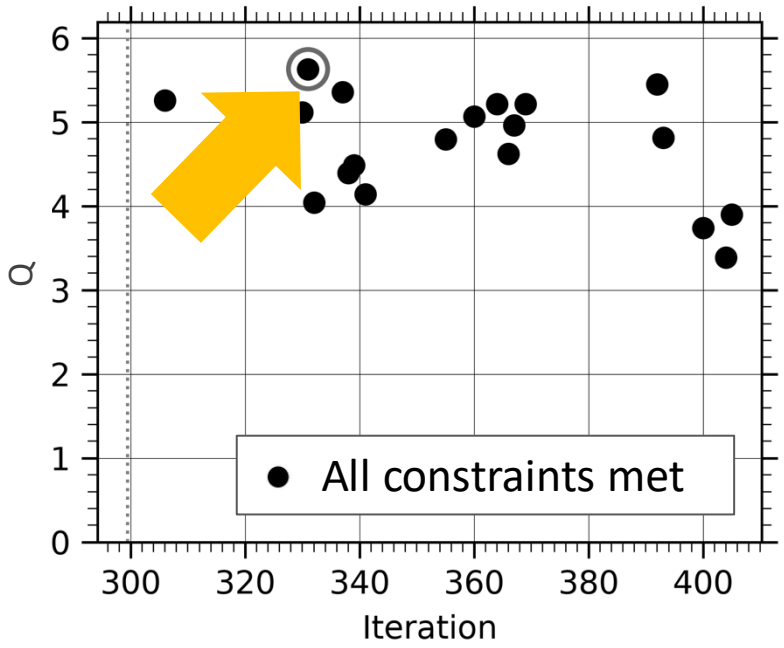
max Q ($f_{Z=3}$, $n_{e,ped}$, κ, δ, ζ, P_{in})

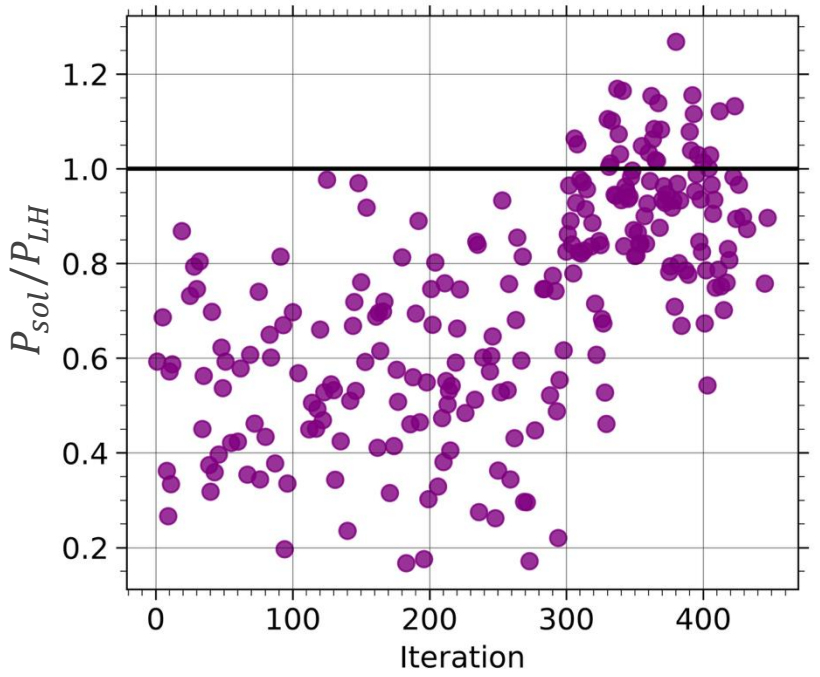
s.t. $\langle n_e \rangle < 0.9\, n_G$

$P_{sol} > P_{LH}$

$P_{fus} < 140$ MW

- Extended Lengyel model to ensure viable core-edge integrated solution (no He ash)
- P_{LH} calculated with $n_e = 0.75 \times \langle n_e \rangle_{H-mode}$ to account for hysteresis
- Consistent with previous literature, key challenge for SPARC PRD is H-mode access

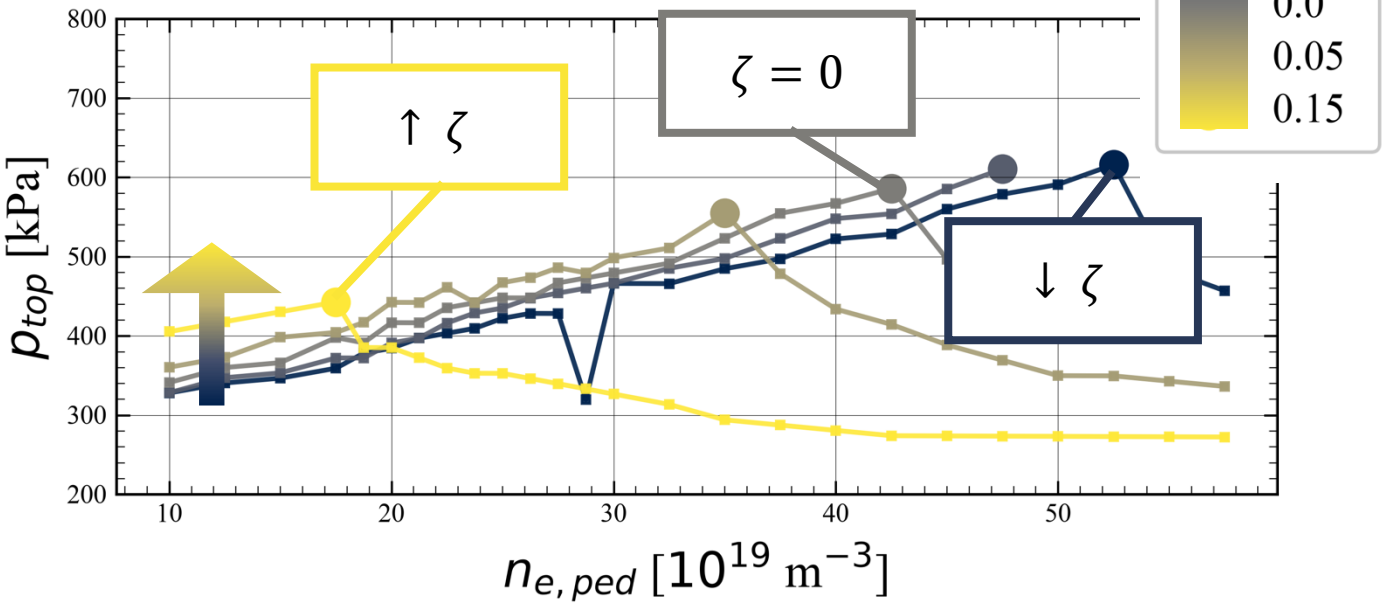




SPARC PRD-like

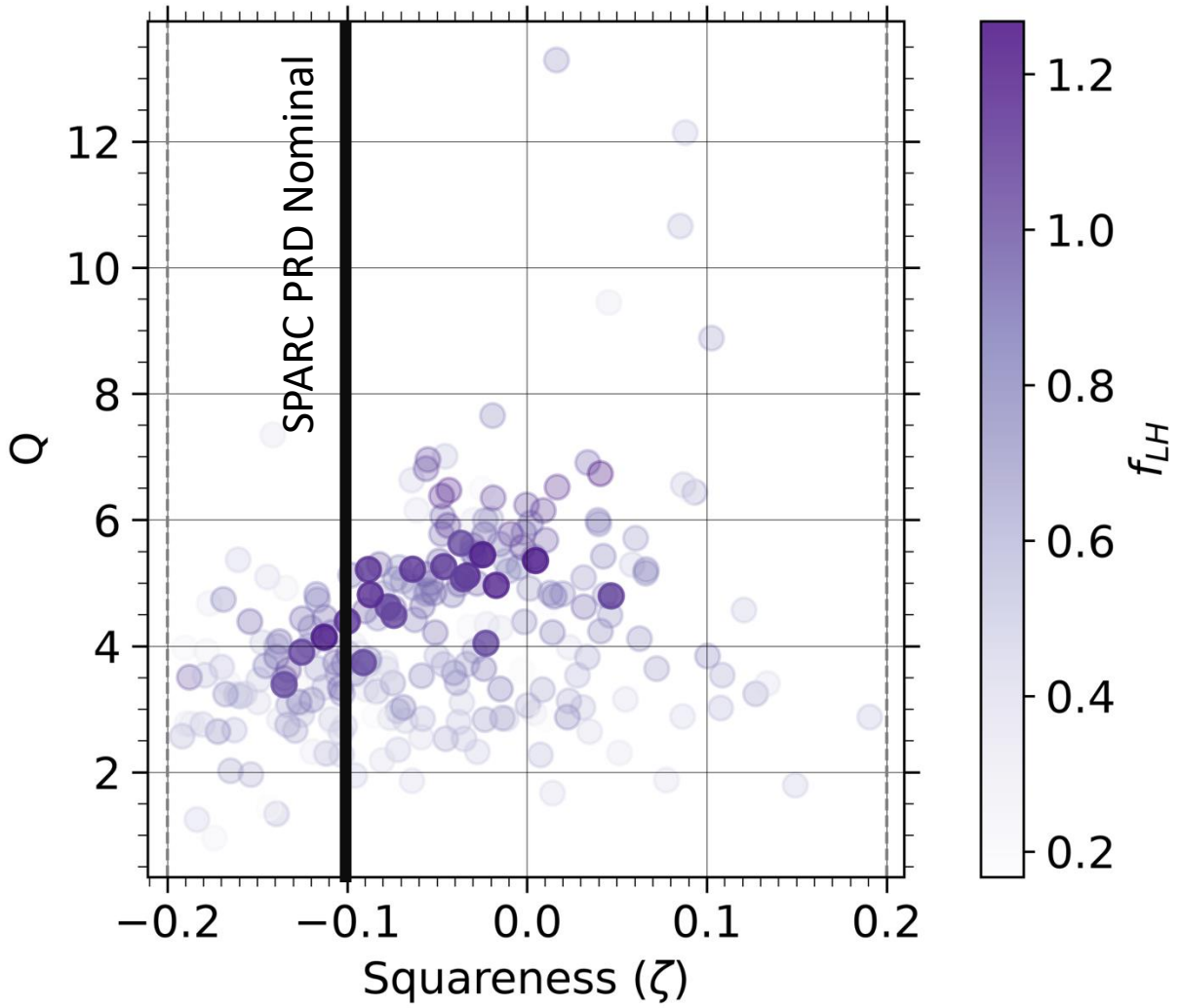
Negative squareness stabilizes ballooning modes in SPARC

- Increased squareness also stabilizes pedestal peeling modes
- Negative squareness stabilizes ballooning modes in SPARC



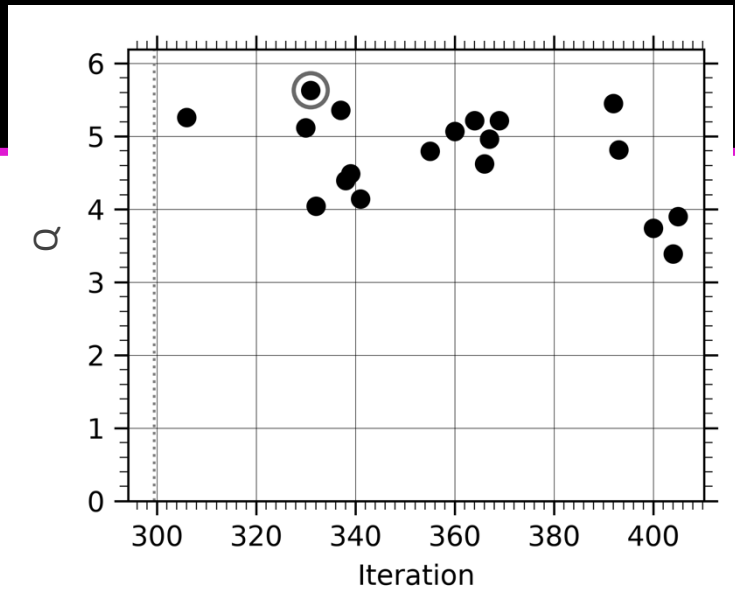
Negative squareness stabilizing ballooning modes in SPARC

- Increased squareness also stabilizes pedestal peeling modes
- Negative squareness stabilizes ballooning modes in SPARC
- Performance degrades rapidly at high positive squareness



Summary: Part Two

A core-edge integrated SPARC PRD scenario with H-mode access achieving Q>5 is identified



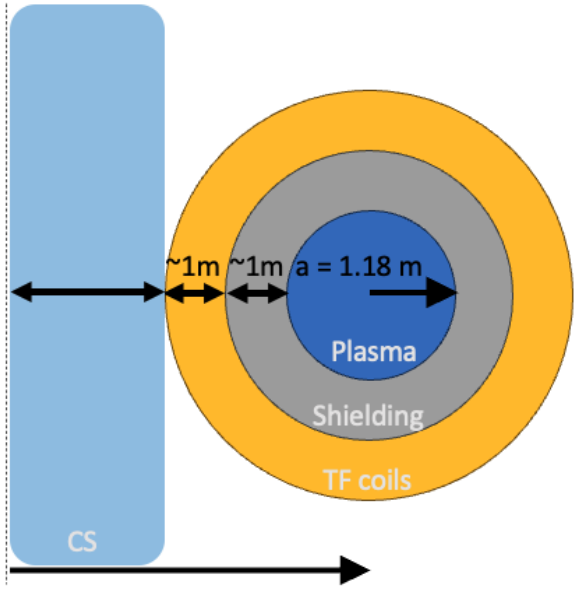
Talk plan

1. Operational optimization (max P_{fus}) of ARC-like device
2. Operational optimization (max Q) of SPARC PRD
3. **Design optimization**

We explore the impact of changing aspect ratio and plasma current

Design Opt

$$\max \; P_{fus}\left(f_{Z=3}, n_{e,ped}, \kappa, \delta, \zeta, I_p, R\right)$$
$$\text{s.t.} \quad \text{constant surface area}$$
$$B_{coil} = 21.5\ \text{T}$$
$$\langle n_e \rangle < 0.95\, n_G$$
$$P_{sol} > P_{LH}$$
$$\tau_{flattop} > 800\ \text{s}$$
$$q95 > 4$$

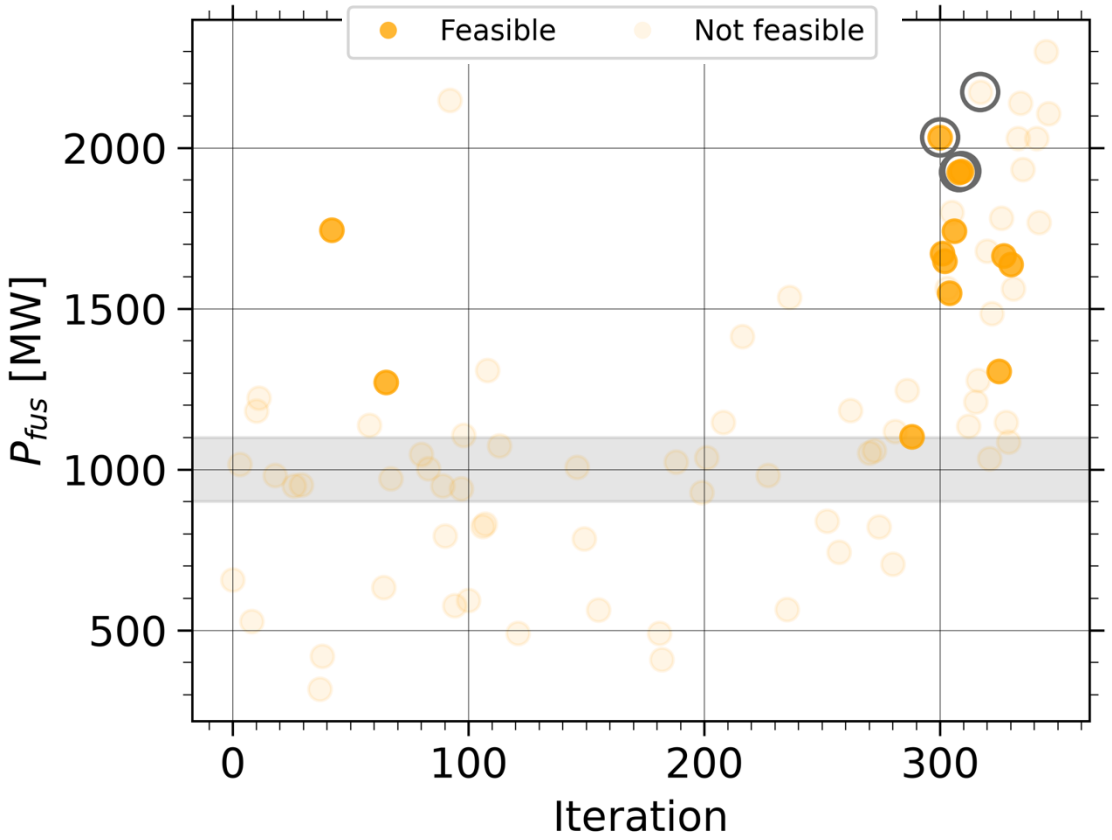


- Plasma current I_p and major radius R are varied
- Plasma surface area is being treated as capital cost proxy, which is held constant
- Minor radius (a) consistent with constant surface area
- B_T consistent with B_{coil}
- Central solenoid radius adjusted assuming constant shielding and TF coil thickness
- Constant maximum elongation with aspect ratio

High-performance core-edge integrated designs successfully identified

Design Opt

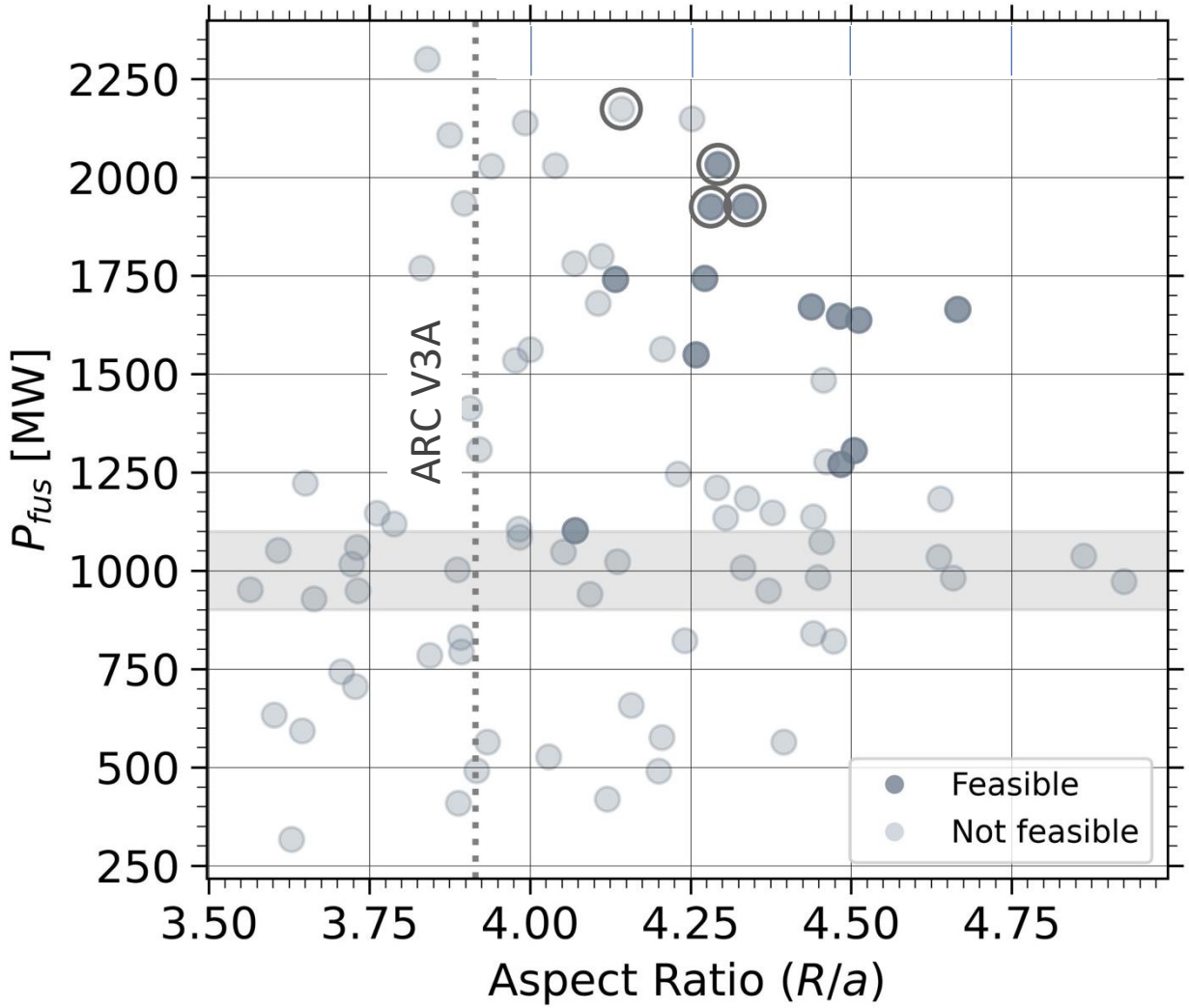
- $P_{fus} > 2$ GW solutions with all constraints met
- Economic figures of merit: fusion power density [MW/m^3]
  and neutron wall load [MW/m^3] (Whyte, J Fusion Energ., 2026) are approximately twice that of ARC V3A



Optimal inputs and performance are highly sensitive to input assumptions. Of importance from this section are trends and what are driving them.

High aspect ratio solutions are favorable for these assumptions

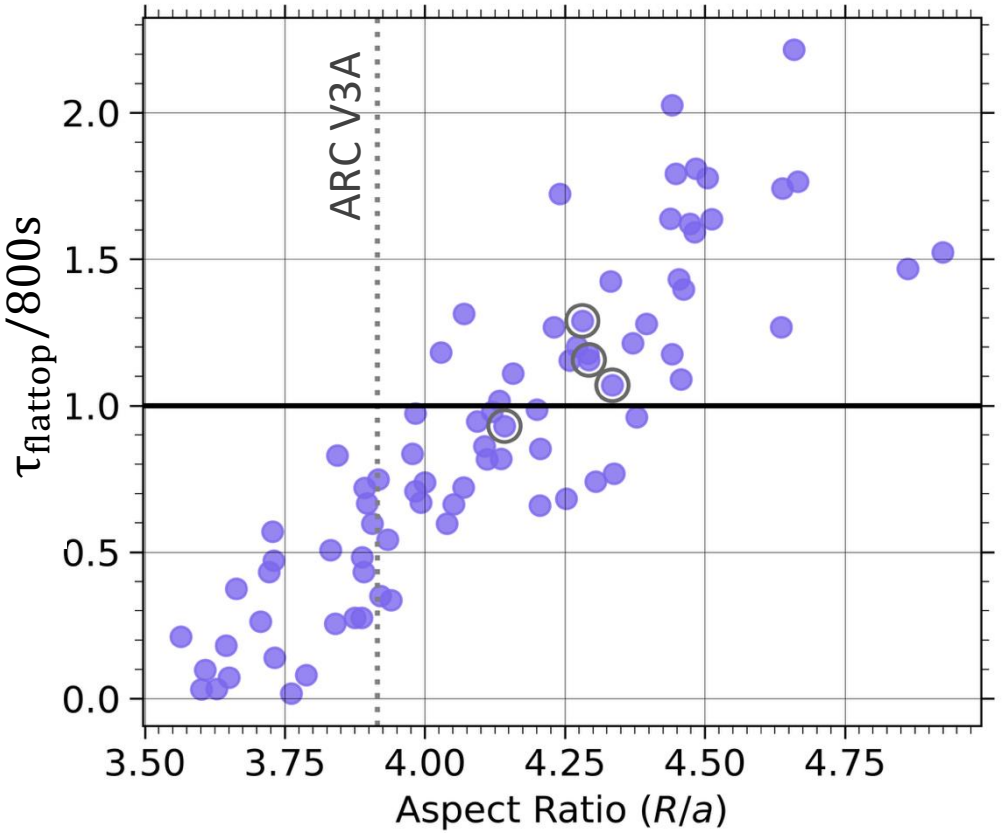
Design Opt



High aspect ratio solutions are favorable for these assumptions

Design Opt

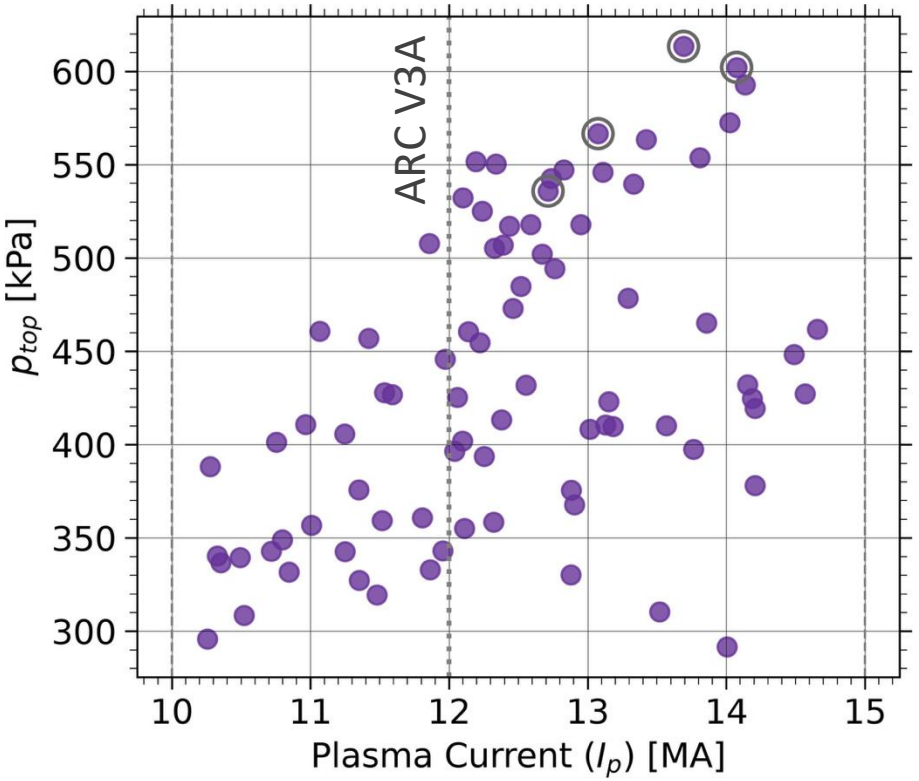
- Fixed $B_{coil} = 21.5\ T$ means higher aspect ratio designs have higher B_T
- Pulse duration requirements, $\tau_{flattop} > 800\ s$, pushes towards higher major radius for central solenoid radius

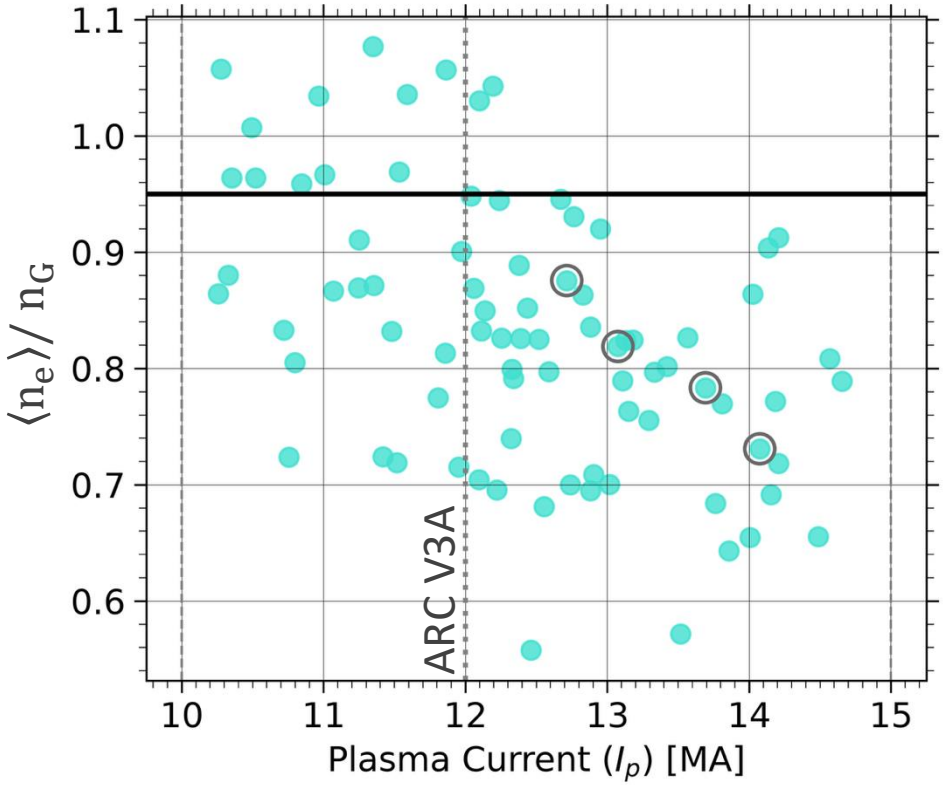


Elevated current is also valuable under these assumptions

Design Opt

- Higher I_p increases pedestal top pressure
- Higher I_p raises Greenwald density limit ($n_G = {I_p}/{\pi a^2}$)

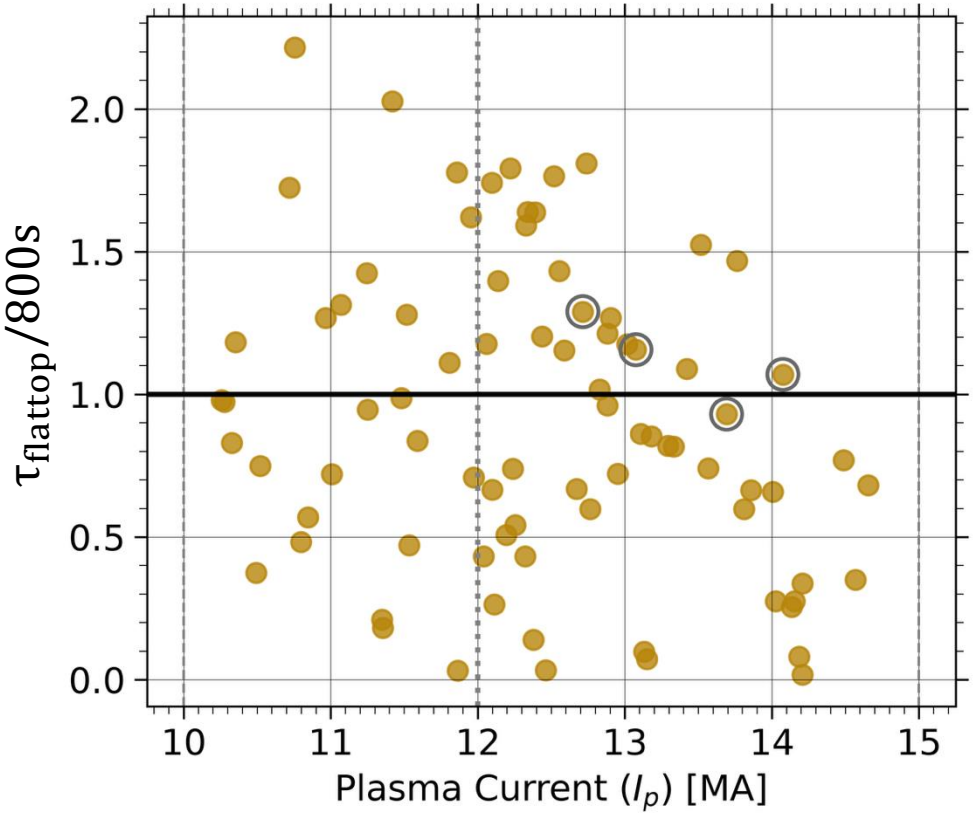


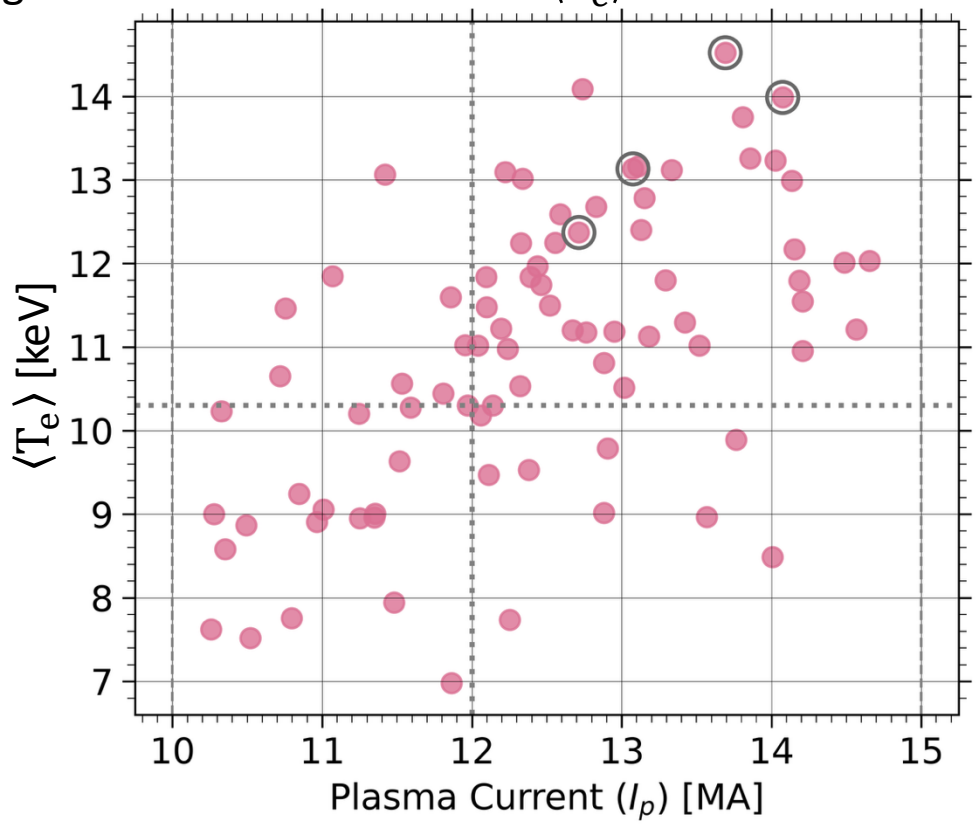


Elevated current is also valuable under these assumptions

Design Opt

- Higher I_p increases pedestal top pressure
- Higher I_p raises Greenwald density limit ($n_G = {I_p}/{\pi a^2}$)
- Pulse duration is not adversely impacted by current again due to due to elevated $\langle T_e \rangle$





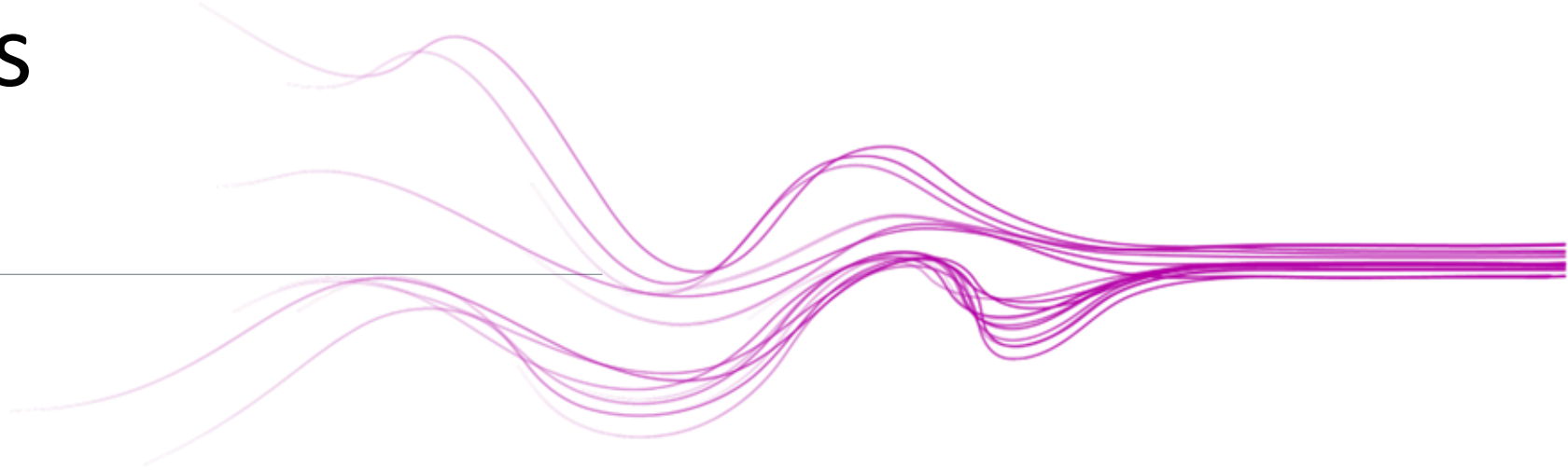
Conclusions: A workflow was developed to perform both operational and design optimization

- **Core-edge integrated** modeling shows the opportunity for fusion power performance improvements for ARC-like devices via operational optimization:
  - **Increases in impurities** offer large benefits to the core and pedestal not captured by empirical models
  - Stronger shaping, including squareness is beneficial
- A core-edge integrated **SPARC PRD** scenario can get at least Q>5 with H-mode access
- **High R/a** solutions are favored due to larger CS and higher B_T given B_{coil}
- High I_p and Z_{eff} values **do not reduce $\tau_{flattop}$** as they drive higher $\langle T \rangle$

- Future work
  - Optimization of SPARC breakeven scenarios
  - Design optimization with varying surface area

Plasma Science & Fusion Center

Reference slides



Reference Slides Contents

- Squareness definition
- Convergence Plots
- 6D Optimization
- 6D Opt Profiles
- 6D Opt 0D Parameters
- 6D Objective Cross Sections
- 6D Lengyel Opt
- Constant elongation opt
- Constant squareness opt
- Howard JPP uncertainty
- Uncertainty Opt: TGLF
- Uncertainty Opt: kEPED
- Uncertainty Opt: fG
- Uncertainty Opt: nesep/neped
- EPED stand alone: β_N & Zeff
- EPED stand alone: Geometry
- EPED stand alone: Ip & s3
- TGLF Stand Alone: Geometry
- TGLF Stand Alone: Squareness
- TGLF Stand Alone: Impurities
- SPARC PRD Opt: Inputs
- SPARC PRD Opt: Outputs
- Design Opt: Inputs
- Design Opt: Constrained Inputs
- Design Opt: Outputs
- Composition Parametric Scan
- Geometry Parametric Scan
- Squareness Parametric Scan